EXPERIMENTALLY QUANTIFYING THE IMPACT OF THERMAL MATURITY ON AROMATICITY AND DENSITY IN KEROGEN

A Thesis

by

ANQI YANG

Submitted to the Office of Graduate and Professional Studies of
Texas A&M University
in partial fulfillment of the requirements for the degree of

MASTER OF SCIENCE

Chair of Committee,	Zoya Heidari
Co-Chair of Committee,	Walter Ayers
Committee Members,	John Killough
	Yuefeng Sun
Head of Department,	A. Daniel Hill

August 2016

Major Subject: Petroleum Engineering

ABSTRACT

Kerogen presents challenges when performing well-log-based petrophysical evaluation in organic-rich mudrocks. Two such challenges are the electrical conductivity of thermally matured kerogen and the lack of reliable estimates of kerogen density. Both challenges are due to the effects of the thermal maturation process on the resistivity and density of kerogen embedded in organic-rich mudrocks. Through thermal maturation, kerogen generates hydrocarbons and evolves from hydrogen-rich organic matter into hydrogen-poor residual matter. Alteration in the chemical structure of kerogen leads to increase in kerogen aromaticity, which can be the reason for unexpectedly low electrical resistivity measurements detected in organic-rich rocks. These low resistivity measurements can lead to underestimates in hydrocarbon reserves. Increase in kerogen aromaticity can also cause increase in kerogen density, which can negatively affect the dependability of porosity and water saturation estimated from well logs. To investigate the impact of thermal maturity on aromaticity, resistivity, and density of kerogen, Rock-Eval pyrolysis, solid-state ^{13}C nuclear magnetic resonance (NMR) spectroscopy, and gas pycnometry were employed. First, kerogen was isolated from organic-rich mudrocks. Select mudrock and isolated kerogen samples were then synthetically matured. Next, aromaticity and electrical resistivity of the mudrock and isolated kerogen samples were evaluated. Lastly, density of the kerogen embedded in the organic-rich mudrocks were estimated.

In investigating the chemical, electrical, and physical properties of kerogen, this thesis demonstrated that aromaticity increased, electrical conductivity increased, and density increased in kerogen as a function of thermal maturity. Through natural maturation, as hydrogen index (HI) decreased from 603 to 36 mg hydrocarbon/g organic carbon, aromaticity of kerogen increased from 0.40 to 0.95. In the isolated kerogen samples from Formation A, resistivity decreased four orders of magnitude from 1.32E+7 to 1.18E+3 Ω·m through synthetic maturation from 150°C to 650°C. In organic-rich mudrocks obtained from four formations, quantifications of kerogen density ranged from 1.20 to 1.78 g/cm^3. Results from this research contribute to a better understanding of organic-rich mudrocks and its embedded kerogen as a function of thermal maturity, which can potentially contribute to the development of dependable well-log-based evaluation of in-situ hydrocarbon saturation and porosity in organic-rich mudrocks.

DEDICATION

This thesis is dedicated to Sarah, my little sister, who is curious, kind, and brave.

ACKNOWLEDGEMENTS

God guides my footsteps. I thank Him for His plan and His blessings.

I thank my parents, Yuanhai Yang and Qimin Lan, for their unconditional love.

I thank Austin Underwood for his support and his encouragements.

I thank Dr. Zoya Heidari for sharing her knowledge, supervising my work, and providing her feedback. I also thank Dr. Walter Ayers, Dr. John Killough, and Dr. Yuefeng Sun for providing their feedback.

Research reported in this thesis was funded by the American Chemical Society and the Joint Industry Research Program on "Multi-Scale Formation Evaluation of Unconventional and Carbonate Reservoirs" at Texas A&M University, jointly sponsored by Aramco Services Company, BHP Billiton, BP, Chevron, ConocoPhillips, and Devon Energy.

I appreciate Eric Carter, Andrew Russell, Mike Shaw, Ryan Zak, and all at W. D. Von Gonten Laboratories for sharing their expertise and making their facilities (e.g., thermal gravimetric analysis, X-ray diffraction, Rock-Eval pyrolysis, gas pycnometer, and high resistance electrometer) available for the experiments conducted in this research.

I appreciate Dr. Vladimir Bakhmoutov and the NMR Facility at Texas A&M University for providing the solid-state ^{13}C NMR spectra.

I appreciate Matthew Wehner for providing the X-ray fluorescence analyses.

I appreciate the comradery of my colleagues in the Multi-Scale Formation Evaluation Research Group.

NOMENCLATURE

f_a	Aromatic Carbon Fraction
FID	Flame Ionization Detector
HI	Hydrogen Index
IR	Infrared
MAS	Magic Angle Spinning
OI	Oxygen Index
ppm	parts per million
NMR	Nuclear Magnetic Resonance
TGA	Thermogravimetric Analysis
TOC	Total Organic Carbon
XRD	X-Ray Diffraction
XRF	X-Ray Fluorescence

TABLE OF CONTENTS

Page

LIST OF TABLES

Page

LIST OF FIGURES

Page

1. INTRODUCTION

This section serves as the introduction to the investigation on the impact of thermal maturity on chemical, electrical, and physical properties of kerogen by highlighting the work of previous researchers through literature review, stating the problem, and listing the objectives.

1.1 Literature Review

Literature review for this research is presented in six topics. The first topic is the origin and chemical structure of kerogen. The next two topics pertain to the geochemical properties of kerogen. These are the evaluation of kerogen with geochemical parameters and the effects of the mineral matrix on geochemical parameters. The final three topics attend to the effects of thermal maturity on chemical, electrical, and physical properties of kerogen. These are the impacts of (a) thermal maturity on the chemical structure of kerogen, (b) increased aromaticity on electrical resistivity in kerogen, and (c) increased aromaticity on density of kerogen.

1.1.1 Origin and Chemical Structure of Kerogen

Kerogen is organic matter embedded in sedimentary rocks (Durand, 1980). It is solid and insoluble in organic solvents (e.g., chloroform).

Three types of kerogen, I, II, and III, can generate hydrocarbons through thermal maturation. Type I kerogen is derived from organic matter deposited in lacustrine settings. Type I kerogen is oil-prone but uncommon, generating less than 3% of hydrocarbon

reserves in the world (Klemme and Ulmishek, 1991). Organic matter deposited in marine settings forms type II kerogen, which can generate both oil and gas. Gas-prone type III kerogen is evolved from terrestrial plants.

Chemical compositions of the three types of kerogen differ in their concentrations of aliphatic and aromatic compounds. In type I kerogen, the concentration of aliphatic compounds is significantly higher than that of aromatic compounds. Both aliphatic and aromatic compounds are present in type II kerogen. In type III kerogen, aromatic compounds dominate the organic fraction and aliphatic compounds are only a minor constituent (Vandenbroucke, 2003).

1.1.2 Evaluation of Kerogen with Geochemical Parameters

Rock-Eval pyrolysis can characterize organic matter embedded in organic-rich mudrocks. Acquired from Rock-Eval pyrolysis, geochemical parameters can quantify the thermal maturity of kerogen in rock samples. Two such parameters are T_{max} and Hydrogen Index (HI). T_{max} characterizes the evolution level of organic matter (Espitalié et al., 1977). HI measures the remaining petroleum potential of kerogen in the rock samples (Vandenbroucke and Largeau, 2007). Both T_{max} and HI can be evaluated in a two-stage process using a Rock-Eval analyzer.

A rock sample undergoes a two-stage process, pyrolysis and oxidation, in a Rock-Eval analyzer. During the pyrolysis stage, the analyzer detects emitted hydrocarbon and carbon dioxide molecules to assess S1, S2, and S3. During the oxidation stage, the analyzer detects emitted carbon molecules to assess S4.

S1 (mg hydrocarbon/g rock) represents the amount of previously generated hydrocarbons that can thermally distill out of the rock sample during pyrolysis, or extractable hydrocarbons (Espitalié et al., 1977). The analyzer assesses S1 at 300°C, when kerogen cracking has yet to occur (Espitalié et al., 1977). As temperature rises above 300°C in the Rock-Eval analyzer, kerogen cracks and produces hydrocarbons, the amount of which equates to S2 (mg hydrocarbon/g rock). Thus, S2 represents the potential of kerogen embedded in the rock sample to generate hydrocarbons, or convertible hydrocarbons (Espitalié et al., 1977). S3 (mg organic carbon dioxide/g rock) indicates the amount of carbon dioxide (CO_2) emitted during pyrolysis (Espitalié et al., 1977). During oxidation, the residual carbons in the rock sample react to emit carbon monoxide (CO) and CO_2, which the analyzer detects to assess S4 (mg carbon/g rock).

Total organic carbon (TOC) is a geochemical parameter that can indicate organic-richness of a rock sample. The Rock-Eval analyzer uses three other geochemical parameters, extractable hydrocarbons (S1), convertible hydrocarbons (S2), and residual carbons (S4), to estimate TOC (Espitalié et al., 1977). Convertible hydrocarbons (S2) and residual carbons (S4) make up the composition of kerogen embedded in a rock sample (Jarvie, 1991). The Rock-Eval analyzer also uses S3 and TOC to estimate Oxygen Index (OI), which is the normalized oxygen content of a rock sample (Espitalié et al., 1977).

T_{max} is the temperature at which S2 reaches its maximum value during pyrolysis. It can represent the thermal maturity of kerogen embedded in a rock sample (Espitalié et al., 1977). T_{max} increases as kerogen thermally matures. However, T_{max} may be inaccurate in rock samples with low S2 values (Peters, 1986). HI can also represent thermal maturity

of kerogen. HI is the ratio of S2 to TOC and corresponds to the hydrogen content of rock samples. Higher HI values indicate higher potentials to generate hydrocarbons. HI decreases as kerogen thermally matures (Peters, 1986; Dellisanti et al., 2010; Nordeng, 2012).

1.1.3 Effects of Mineral Matrix on Geochemical Parameters

With the advent of pyrolysis technologies, including Rock-Eval analyzer, the thermal maturity of kerogen embedded in rock samples has been determined rapidly without the isolation of kerogen. As stated above, this kerogen aging technique is based on geochemical parameters (i.e., T_{max} and HI) assessed through the analysis of rock samples. Multiple researchers (Katz, 1983; Clementz, 1978; Espitalié et al., 1980; Horsfield and Douglas, 1980) have suggested that this technique yields inaccurate results. Furthermore, these results may not be compared to results acquired from isolated kerogen samples.

Clementz (1987) suggested that S2 values obtained from rock samples may include hydrocarbons generated from the cracking of solid bitumen and heavy hydrocarbons, as well as from kerogen cracking. Thus, the S2 and HI values obtained from rock samples may be inaccurate. This concern can be addressed by treating the rock samples with an organic solvent (e.g., chloroform) prior to analysis. Another concern is the effects of minerals on the yield of hydrocarbons from kerogen cracking and consequently, the quantification of kerogen thermal maturity from pyrolysis (Espitalié et al., 1980; Horsfield and Douglas, 1980; Katz, 1983). This concern can be addressed by treating the rock

samples with acids (e.g., HCl and HF). This concern is further discussed with experiments conducted by Katz (1983).

Katz (1983) investigated the validity of HI values obtained with Rock-Eval pyrolysis on rock samples by analyzing isolated kerogen samples mixed with calcite and Ca-montmorillonite. In these experiments, Katz (1983) observed higher HI values in the calcite mixtures as compared to the Ca-montmorillonite mixtures. This observation demonstrates that the presence of minerals affects the assessment of the geochemical parameter HI. Katz (1983) also suggested that the mineral matrix has a retention capacity for hydrocarbons regardless of organic content. This retention capacity may affect the assessment of HI. These observations solidify the need to demineralize rock samples prior to assessing the geochemical properties of kerogen embedded in organic-rich mudrocks.

From the work of multiple researchers (Katz, 1983; Clementz, 1978; Espitalié et al., 1980; Horsfield and Douglas, 1980), it is evident that minerals can affect the assessment of geochemical parameters by diluting the existing organic matter and retaining the generated hydrocarbons. Thus, in order to accurately evaluate geochemical parameters of kerogen embedded in organic-rich mudrocks to precisely quantify the thermal maturity of kerogen, kerogen must be isolated from the mineral matrix of organic-rich mudrocks.

1.1.4 Impact of Thermal Maturity on Chemical Structure of Kerogen

From organic matter deposition to hydrocarbon generation, the thermal maturation process of source rocks comprises of three stages, diagenesis, catagenesis, and metagenesis (Tissot et al., 1974). Source rocks can be classified as thermally immature,

mature, or post-mature based on the fluids generated. Immature rocks have yet to generate hydrocarbons and have been through the diagenesis and early catagenesis stages. Mature and post-mature rocks generate oil and gas, respectively. As the metagenesis stage continues in post-mature rocks, their hydrogen content depletes and gas generation ceases (Tissot et al., 1974). Rock samples obtained from sources rocks (e.g., organic-rich mudrocks) contain both hydrocarbons generated previously and kerogen that has yet to react completely.

Kerogen produces bitumen, which is soluble in organic solvents (e.g., chloroform), and hydrocarbons upon thermal maturation and its chemical composition changes as hydrogen-rich organic matter converts into hydrogen-poor residual matter. The hydrogen content of kerogen depletes and its reactive carbons evolve into dead carbons as a function of thermal maturity until its hydrogen concentration is negligible and its composition is dominated by dead carbons (Tissot et al., 1974; Baskin, 1997).

With regards to the chemical structure of kerogen, thermal maturation converts aliphatic moieties into aromatic moieties (Vandenbroucke, 2003), which increases the aromaticity of kerogen. An investigation by Wei et al. (2005) demonstrated that aromaticity and aromatic cluster size both increase as a function of thermal maturity in isolated kerogen samples. Aromatic cluster size represents the number of aromatic rings fused together, this parameter corresponds to the amount of aromatic bridgehead carbons. Aromatic bridgehead carbons join three aromatic rings by bonding to other aromatic carbons (Mao et al., 2010). Mao et al. (2010) suggested that aromaticity, amount of aromatic carbons, and ratio of aromatic to aliphatic compounds all increase through

thermal maturation. Mao et al. (2010) also showed that aromatic cluster size increases slightly as well. Walters et al. (2014) detected turbostratic carbon nanostructures in demineralized and whole shale rock samples using high resolution transmission electron microscopy (HRTEM). Turbostratic carbon nanostructures are composed of basic structural units (BSU) with sp^2 carbon networks, which are formed through the carbonization process that occurs with thermal maturation of kerogen (Walters et al., 2014). The increase in aromaticity, aromatic cluster size, and frequency of turbostratic carbon nanostructures as a function of thermal maturity can be reasons for the high electrical conductivity of highly mature shales (Walters et al., 2014).

1.1.5 Impact of Increased Aromaticity on Electrical Resistivity in Kerogen

To understand the effects of thermally matured kerogen on electrical resistivity measurements on organic-rich mudrocks, it is necessary to consider the impact of thermal maturity on aromaticity in kerogen. The thermal maturation process increases the aromaticity of kerogen embedded in organic-rich mudrocks, which occurs in conjunction with increases in aromatic cluster size and frequency of turbostratic carbon nanostructures. The increase in aromatic cluster size corresponds to the increase in degree of condensation among aromatic sheets in kerogen (Wei et al., 2010). The increases in the aromatic cluster size and frequency of turbostratic carbon nanostructures lead to the formation of electrically conductive macroscopic pathways due to two phenomena, (a) physical contact among the nanostructures and (b) condensation among aromatic/graphene sheets (Walters et al., 2014). Furthermore, experiments conducted by Northrop and Simpson (1956)

suggested a tendency towards higher electron mobility in larger aromatic hydrocarbon molecules than in their smaller counterparts.

Previous researches stated that solid-state ^{13}C nuclear magnetic resonance (NMR) spectroscopy is the only technology capable of quantifying the chemical structure of kerogen (Vandenbroucke, 2003; Wei et al., 2005) through the estimations of aliphatic and aromatic carbon bonds and the assessment of aromaticity. Solid-state ^{13}C NMR spectroscopy can quantify aromaticity by assessing relative amounts of aliphatic and aromatic compounds in organic-rich mudrock and isolated kerogen samples.

1.1.6 Impact of Increased Aromaticity on Density of Kerogen

As aromatic cluster size and aromaticity increase, the amount of hydrogen-rich molecules decreases, which can lead to an increase in the density of kerogen. Previous publications showed that the density of kerogen varies as a function of thermal maturity (Van Krevelen, 1961; Kinghorn and Rahman, 1983; Okiongbo et al., 2005). According to Van Krevelen (1961), density of vitrinite, a type of maceral present in coals and kerogens, decreases then increases as its thermal maturity increases. This phenomenon is due to first a depletion in oxygen content and then a depletion in hydrogen content. The initial decrease in the density of vitrinite occurs in thermal maturation levels at which hydrocarbons are generated. As vitrinite evolves entirely into dead carbons, its density increases and reaches that of graphite, 2.25 g/cm^3 (Van Krevelen, 1961). According to Kinghorn and Rahman (1980, 1983), density of kerogen increases from type I, to type II, and then to type III kerogen.

A previous publication by Okiongbo et al. (2005) demonstrated that the density of oil-prone, type II kerogen, isolated from the Upper Jurassic Kimmeridge clay formation, increases as its thermal maturity increases. In thermal maturation levels below those at which hydrocarbon is generated, kerogen density remains constant with respect to HI. At higher thermal maturity levels, kerogen density increases as HI decreases during and after hydrocarbon generation. Okiongbo et al. (2005) also showed that as T_{max} increases above 440°C, the density of isolated kerogen samples increases.

Increase in the density of kerogen as a function of thermal maturity is due to reduction in alkyl carbons and aromatization in aliphatic carbons (Patience et al., 1992; Okiongbo et al., 2005). Patience et al. (1992) evaluated the chemical structure of kerogen extracted from the Kimmeridge clay formation. Their results demonstrate that kerogen aromaticity increases as thermal maturity increases during and after hydrocarbon generation. Increase in aromaticity is due to two phenomena. First, alkyl carbons attached to aromatic clusters detach for the purpose of hydrocarbon generation and thus, the concentration of aromatic carbons increases. Second, during hydrocarbon generation, aromatization reactions occur to form new aromatic rings and thus, the size of aromatic clusters increases (Patience et al., 1992). Both phenomena promote increase in kerogen aromaticity, which leads to graphitization of kerogen. Thus, the density of kerogen approaches that of graphite, 2.25 g/cm^3 (Van Krevelen, 1961).

1.2 Statement of Problem

Kerogen embedded in organic-rich mudrocks presents challenges when performing well-log-based evaluation of petrophysical properties in organic-rich mudrocks, such as porosity and in-situ hydrocarbon saturation. Two such challenges are the electrical conductivity of thermally matured kerogen and the lack of reliable estimates of kerogen density. Both challenges are due to the impact of thermal maturity on chemical, electrical, and physical properties in kerogen. As kerogen matures, hydrocarbons are generated and its chemical structure is altered. Alterations in the chemical structure of kerogen lead to increase in its aromaticity, which can cause measureable low electrical resistivity and high density in thermally matured kerogen. Previous researchers have investigated the chemical structure of kerogen as a function of thermal maturity and demonstrated that kerogen aromaticity increases upon thermal maturation (Wei et al., 2005; Mao et al., 2010).

Thermally matured kerogen is one of the electrically conductive components (e.g., saline water, clay minerals, and pyrite) in organic-rich mudrocks, which potentially influences electrical conductivity measurements. Interpretation of electrical resistivity logs influenced by such kerogen can result in overestimation of water saturation (Figure 1) and thus, underestimation of hydrocarbon reserves. Previous publications have documented that electrical resistivity decreases significantly as thermal maturity increases in organic-rich mudrocks (Rajeshwar et al., 1980; Duba, 1983; Meng et al., 2012; Firdaus and Heidari, 2015). However, the connection between aromaticity and electrical

conductivity in kerogen-bearing mudrock and isolated kerogen has yet to be analyzed and quantified simultaneously.

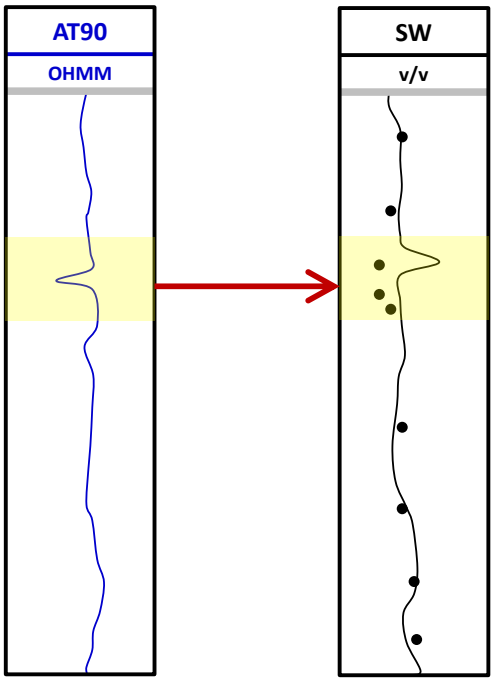

Figure 1: Impact of thermally matured kerogen on estimates of water saturation.

Reliable estimation of kerogen density is a requirement for dependable well-log-based petrophysical evaluation of organic-rich mudrocks. Inaccuracies in estimates of kerogen density can negatively influence assessments of porosity, mineralogy, and water saturation in organic-rich mudrocks. For instance, underestimates in kerogen density can lead to underestimates in porosity (Figure 2). Although previously developed techniques have quantified kerogen density using core measurements, the density of kerogen and the connection between density and thermal maturity of isolated kerogen have yet to be quantified in a variety of organic-rich mudrocks.

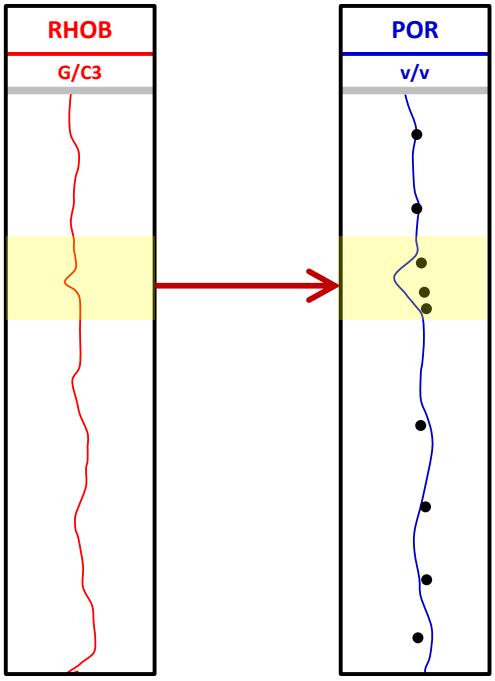

Figure 2: Impact of thermally matured kerogen on estimates of porosity.

1.3 Objectives

To potentially improve the dependability of petrophysical properties estimated from well logs of organic-rich mudrocks, it is essential to better understand the chemical, electrical, and physical properties of thermally matured kerogen. Thus, the objectives of this thesis are to experimentally quantify (a) aromaticity in isolated kerogen samples, (b) electrical resistivity in organic-rich mudrock and isolated kerogen samples, and (c) density of kerogen embedded in a variety of organic-rich mudrock samples, as a function of thermal maturity.

To fulfill this objective, I first obtain isolated kerogen samples from four organic-rich mudrock formations (i.e., Formation A, B, C, and D) with different origins. Kerogen embedded in these four formations vary significantly in thermal maturity. Furthermore, I

synthetically mature mudrock and isolated kerogen samples from select formations. I then perform direct measurements of thermal maturity, aromaticity, and electrical resistivity on both naturally- and synthetically-matured mudrock and isolated kerogen samples. Lastly, I estimate the density of kerogen embedded in all four formations.

2. METHOD

This section describes the method used for investigating the impact of thermal maturity on chemical, electrical, and physical properties of kerogen. The purpose is to detail the experiments conducted, technologies employed, and procedures followed. Figure 3 illustrates the workflow designed in this thesis.

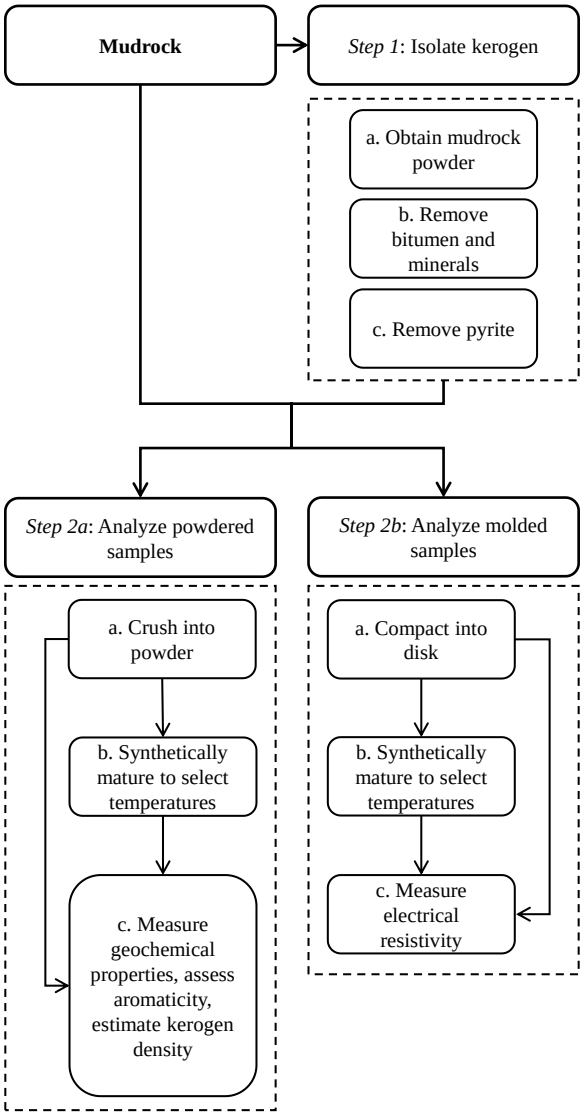

Figure 3: Workflow to quantify chemical, electrical, and physical properties of kerogen.

First, I perform successive physical and chemical treatments to isolate kerogen samples from organic-rich mudrocks. Next, I prepare powdered and molded samples for different measurements. I synthetically mature mudrock and isolated kerogen samples to select heat treatment temperatures. The technologies employed to measure thermal maturity, aromaticity, electrical resistivity, and density are Rock-Eval pyrolysis, solid-state ^{13}C NMR spectroscopy, high resistance measurements, and gas pycnometry. I quantify thermal maturity of non-heated and heat-treated mudrock and isolated kerogen samples using geochemical parameters evaluated with Rock-Eval pyrolysis. To measure variation in aromaticity of samples with different thermal maturity levels, I use estimates of relative amounts of aliphatic and aromatic components derived from solid-state ^{13}C NMR spectroscopy. Next, I measure electrical resistivity of the mudrock and isolated kerogen samples. I then measure the density of each isolated kerogen sample with gas pycnometry. Next, I use data collected with X-ray fluorescence (XRF) analysis to estimate the concentration of pyrite in each isolated kerogen sample. Finally, I correct the measured density for the impact of pyrite to estimate the true density of kerogen. The following subsections outline each step of the introduced workflow (Figure 3) in detail.

2.1 Kerogen Isolation

To accurately quantify the thermal maturity of kerogen, it is necessary to isolated kerogen from the mineral matrix of organic-rich mudrocks. To prepare isolated kerogen samples for analysis, I follow a procedure with three major steps: (1) obtain mudrock powder; (2) remove bitumen and minerals; and (3) remove pyrite.

2.1.1 Step 1: Obtain Mudrock Powder

Figure 4 shows the process to obtain mudrock powder. I obtain mudrock powder by crushing mudrock samples using a mortar and pestle and then sieving the crushed mudrocks using a mechanical sieve equipped with 8, 16, 20, 50, 100, and 170 mesh trays. From the bottom of the mechanical sieve, I obtain mudrock powder, which consists of particles that are less than 88 microns in size. This powder is used in chemical treatments.

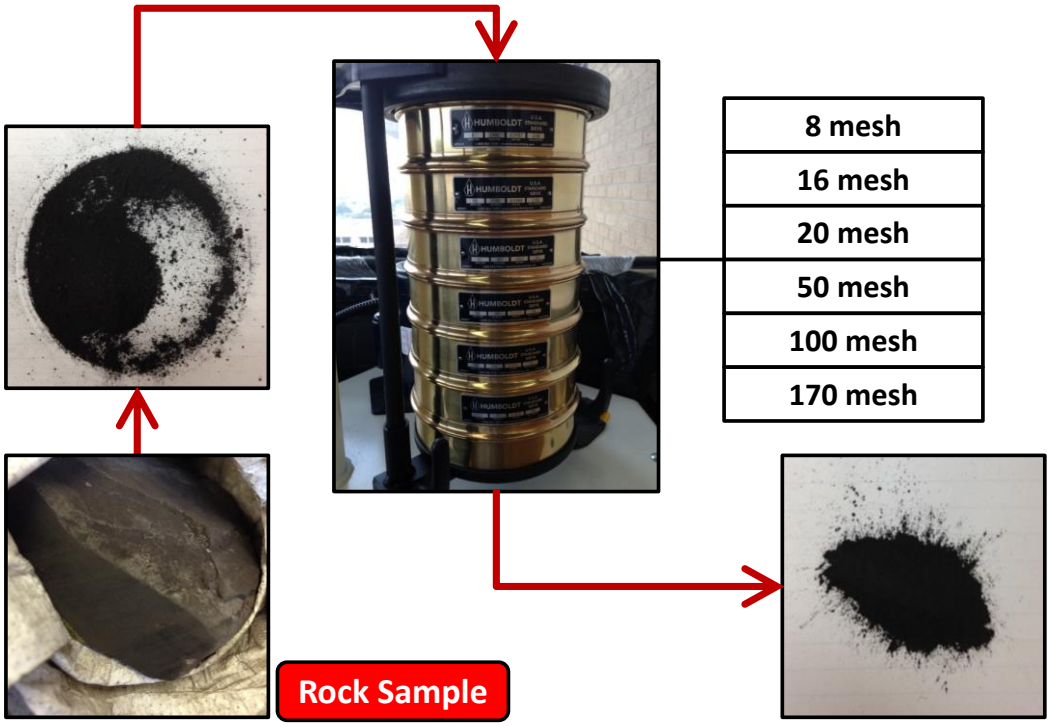

Figure 4: Process to obtain mudrock powder.

2.1.2 Step 2: Remove Bitumen and Minerals

I remove bitumen and minerals by applying a procedure introduced by Durand and Nicaise (1980) and detailed by Vandenbroucke (2003). This procedure consists of multiple chloroform, hydrochloric (HCl) acid, and hydrofluoric (HF) acid treatments. Chloroform

is an organic solvent commonly used in kerogen isolation procedures to remove free hydrocarbons and bitumen. HCl and HF acids can remove carbonates and silicates, respectively. Specifically, the reaction between HCl acid and calcium carbonate is

$$2HCl(aq) + CaCO_3(s) \rightarrow CaCl_2(aq) + CO_2(g) + H_2O(l). \quad (1)$$

HF acid can react with silicates. Specifically, the reaction between HF acid and silicon dioxide is

$$4HF(aq) + SiO_2(s) \rightarrow SiF_4(aq) + 2H_2O(l). \quad (2)$$

To remove bitumen (Figure 5), I combine mudrock powder and chloroform in a glass beaker. Next, a stir bar and magnetic stirrer agitates this mixture for 30 minutes. I then immerse the bottom of the beaker in an ultrasonic bath. After repeating the above two steps (i.e., stir and immerse) twice, I filter the mixture and allow the residue to dry until it naturally separates from the filter paper.

Next, I scrap this residue off of the filter paper into a plastic beaker. To remove minerals (Figure 6), I perform successive 6M HCl acid and 48% HF acid treatments. Each treatment includes combining the residue and acid in a plastic beaker, stirring the mixture for 4 to12 hours, filtering the mixture, and rinsing the filtrand with warm distilled water at least four times. After two HF acid treatments, the final step is to perform additional HCl acid and chloroform treatments in order to prevent deposition of complex fluorides and remove any newly freed bitumen, respectively. The final residue is free of bitumen, carbonates, and silicates. It is composed of organic matter and heavy minerals (i.e., primarily pyrite).

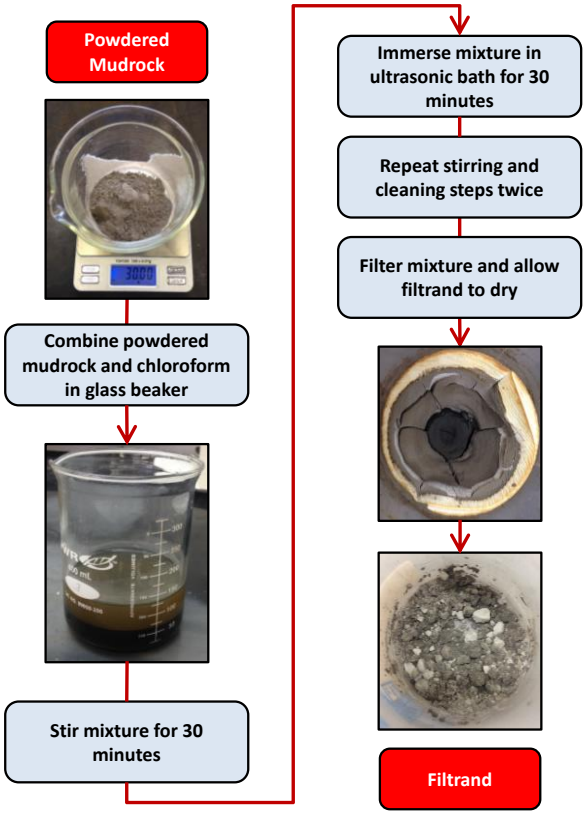

Figure 5: Process to remove bitumen.

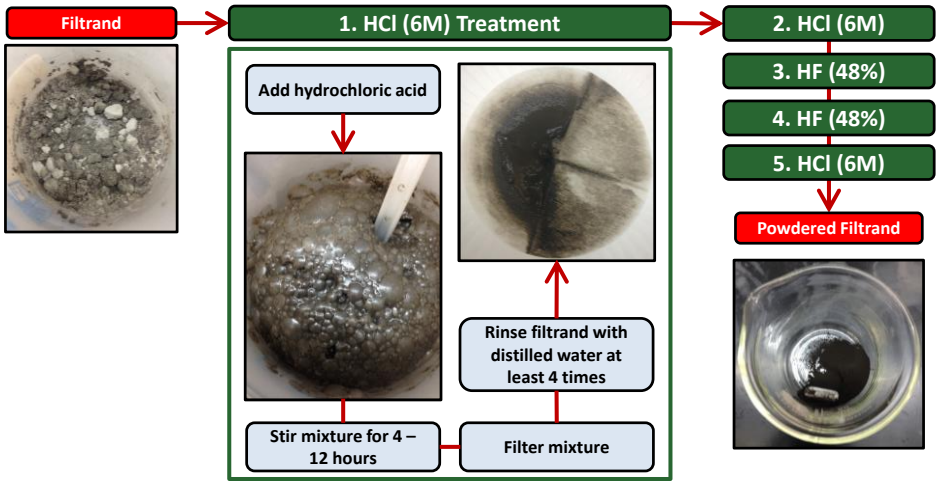

Figure 6: Process to remove minerals.

2.1.3 Step 3: Remove Pyrite

I remove pyrite and other heavy minerals by applying a density-based separation technique used by Kinghorn and Rahman (1980, 1983). Figure 7 illustrates this technique, which utilizes zinc bromide ($ZnBr_2$) solution. $ZnBr_2$ is the most suitable heavy liquid for density separation in sedimentary rocks (Kinghorn and Rahman, 1980). I use a $ZnBr_2$ solution that is composed of 73-77 wt% $ZnBr_2$ and water. The solution is a clear, colorless, and viscous liquid with a density of 2.30 to 2.51 g/cm^3, which is suitable for removing pyrite as the density of pyrite is significantly higher than that of the kerogen solid particles or the $ZnBr_2$ solution.

To remove pyrite, I grind the treated sample (i.e., treated with chloroform, HCl acid, and HF acid) into a very fine powder to enhance contact between solid and solution. Next, I stir the powder into the $ZnBr_2$ solution. I then pour this mixture into glass test tubes and use a centrifuge to spin the test tubes at 2000 rpm for 20 minutes (Ebukanson and Kinghorn, 1985). The separation between a float fraction and a sink fraction should be clearly visible inside each test tube. The float fraction consists of kerogen solids and the sink fraction contains heavy minerals. If separation is not visible, it is necessary to repeat the centrifuge step. I decant the float fraction of each test tube. Finally, I filter, rinse, and dry the isolated kerogen.

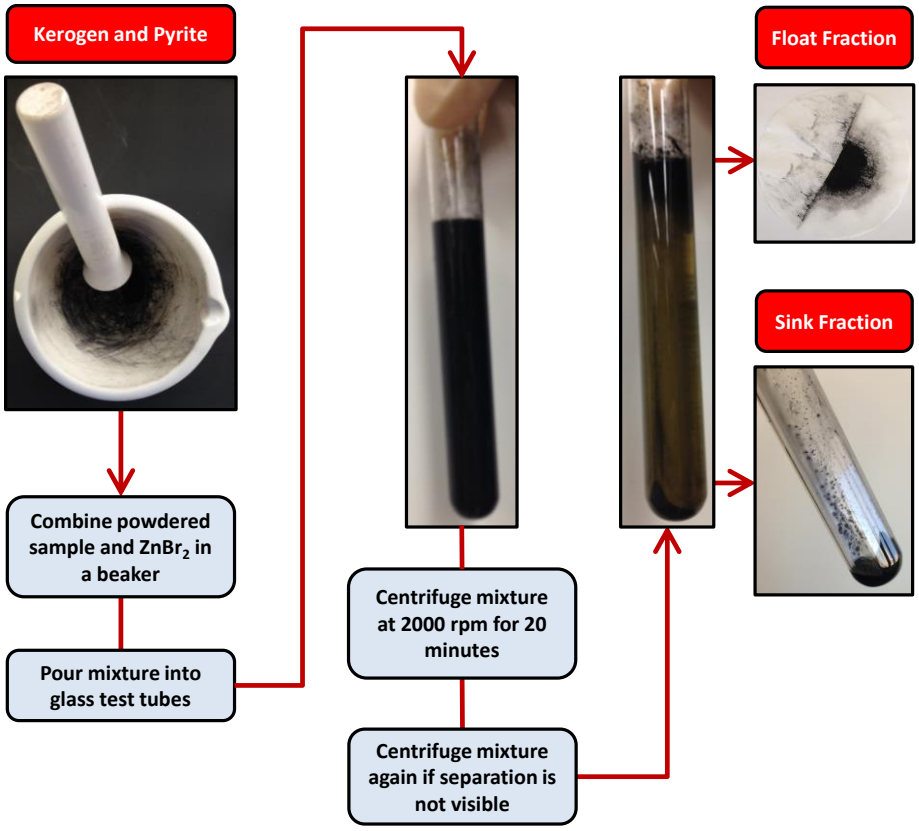

Figure 7: Process to remove pyrite.

2.1.4 Ensure Isolated Kerogen Quality

To confirm the elimination of minerals and pyrite, I employ XRF analysis to measure elemental compositions of powdered mudrock samples and kerogen isolated from such samples. XRF analysis is non-destructive to the samples and can detect and quantify the weight concentrations of elements ranging from magnesium to uranium in solid samples. In the XRF instrument, high energy X-rays are emitted into a powdered sample. These X-rays may detach an electron from the inner orbital shell of an atom. If this occurs, the atom is destabilized and must drop an electron from a higher energy state to the lower

energy state in order to fill the void. The energy emitted by this drop is detected and processed by the XRF instrument. In the resulting spectrum, the concentrations of elements present in the analyzed sample can be evaluated based on the observed peak energies and their respective intensities.

Results from XRF analysis indicate significant reductions in silicon, potassium, calcium, and aluminum. Additionally, I employ Rock-Eval pyrolysis to measure organic content before and after performing kerogen isolation. Results from Rock-Eval pyrolysis demonstrate significant increases in TOC of the isolated kerogen samples as compared to the powdered mudrock samples.

2.1.5 Sample Compaction

After confirming the absence of minerals in the isolated kerogen samples, I prepare mudrock and isolated kerogen samples in forms suitable for direct measurements of thermal maturity, aromaticity, electrical resistivity, and density. The high resistance meter requires compacted samples whereas powdered samples can be used for the rest of the measurements. For the case of the high resistance measurements, I compact mudrock and kerogen powders into disks of 1.7 to 2.5 mm in thickness and 4.9 to 5.4 cm^2 in cross-sectional area. Next, I proceed to synthetically mature powdered and molded mudrock and isolated kerogen samples. Figure 8 shows an image of an organic-rich mudrock from Formation A and images of kerogen isolated from such mudrock, in powdered and molded forms.

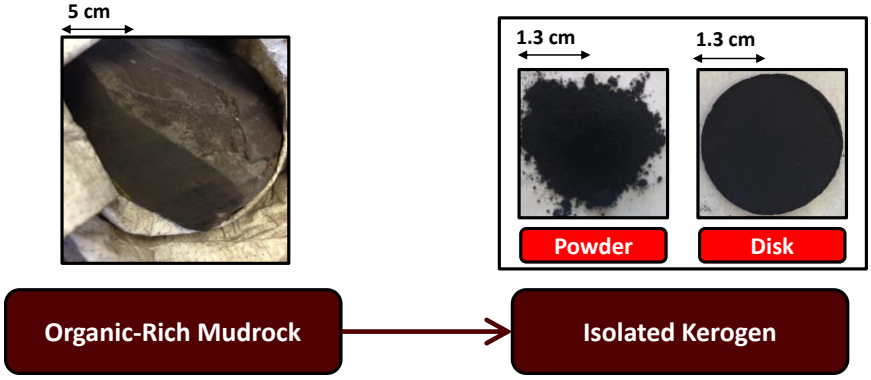

Figure 8: Images of organic-rich mudrock and isolated kerogen samples.

2.2 Synthetic Maturation

In addition to using samples from different formations at different thermal maturation levels, I perform experiments on synthetically matured mudrock and isolated kerogen samples. These samples are matured to select heat treatment temperatures. According to Vandenbroucke (2003), short durations at high temperatures in the laboratory can induce the thermal cracking of kerogen which occurs during long durations at low temperatures in the subsurface. Thus, synthetic maturation experiments conducted at high temperatures can be used to replace natural maturation (Vandenbroucke, 2003).

I use a thermogravimetric analysis (TGA) instrument to synthetically mature powdered mudrock and isolated kerogen samples in an inert environment with nitrogen gas flowing at 100 mL/minute. The step-by-step synthetic maturation procedure includes (a) maintaining the sample at room temperature for 20 minutes, (b) heating the sample at 4^{o}C/minute to the target heat treatment temperature, (c) maintaining the sample at the target heat treatment temperature for 20 minutes, and (d) air cooling for 45 minutes. To

synthetically mature molded mudrock and isolated kerogen disks, I use a heater inside an X-ray diffraction (XRD) instrument. The heating procedure consists of three steps, (a) maturing the disk at 4°C/minute from room temperature to the target heat treatment temperature, (b) isothermally heating the disk for one hour, and (c) decreasing the temperature at 30°C/minute to 30°C. I isothermally heat each disk for an additional hour to ensure that its entire volume reaches the target temperature.

2.3 Rock-Eval Pyrolysis

Rock-Eval pyrolysis can characterize organic matter embedded in rock samples (Espitalié et al., 1977; Vandenbroucke, 2007). In this research, the primary purpose of employing Rock-Eval pyrolysis is to quantify thermal maturity of mudrock and isolated kerogen samples. I use the geochemical parameter HI to fulfill this purpose. To obtain HI, I apply different pyrolysis techniques on mudrock and isolated kerogen powders. The technique designed for mudrock samples requires approximately 60 mg of mudrock powder per analysis whereas the pure organic matter technique requires less than 10 mg of isolated kerogen powder. This decrease in sample weight (Vandenbroucke and Largeau, 2007) is to avoid saturating the flame ionization detector (FID). Figure 9 shows the Rock-Eval analyzer employed in this research.

Figure 9: Rock-Eval analyzer of W. D. Von Gonten Laboratories.

The step-by-step pyrolysis procedure under nitrogen gas flow includes (a) rapidly heating the sample to 300°C, (b) isothermally heating the sample at 300°C for several minutes, and (c) heating the sample at 25°C/minute to 800°C. During pyrolysis, a FID measures any hydrocarbons generated by the sample. The Rock-Eval analyzer uses this information to assess geochemical parameters S1 and S2 (Espitalié et al., 1977). Next, the oxidation stage is initiated. The oxidation stage is under oxygen gas flow and consists of heating the sample at 20°C/minute up to 850°C. During both pyrolysis and oxidation, infrared (IR) detectors measure emitted CO and CO_2 gases (Espitalié et al., 1977). Lastly, the Rock-Eval analyzer calculates and outputs the geochemical parameters (i.e., HI, T_{max}, S1, and S2) of each isolated kerogen sample.

2.4 Solid-State ^{13}C NMR Spectroscopy

Solid-state ^{13}C NMR spectroscopy can identify carbon-bearing compounds present in powdered samples and thus, facilitate analysis of chemical structures in organic matter. This technology is employed to identify and quantify aliphatic and aromatic compounds present in non-heated and heat-treated mudrock and isolated kerogen samples in order to assess aromaticity in such samples.

A 400 MHz spectrometer equipped with 2.5 to 7.0 mm rotors spinning at 4.4 to 10.0 kHz is used to obtain solid-state ^{13}C direct excitation magic angle spinning (MAS) NMR spectra. In the MAS experiments, contact time of radio frequency (RF) pulses is 4-5 microseconds with relaxation delay of 6 seconds. It is necessary to perform approximately 20,000 cycles to obtain a powder spectrum of a mudrock or isolated kerogen sample. A powder spectrum represents a compilation of signals, each at a specific chemical shift. In these experiments, chemical shifts refer to tetramethylsilane (TMS). The outcome of these measurements indicates relative amounts of aliphatic and aromatic compounds present in the mudrock or isolated kerogen samples. The measured values are used to quantify the aromatic carbon fraction (f_a) parameter, which is commonly referred to as aromaticity and given by

$$f_a = \frac{A_{aromatics}}{A_{aliphatics} + A_{aromatics}}, \tag{3}$$

where $A_{aromatics}$ is the integrated intensity in the aromatic region and $A_{aliphatics}$ is the integrated intensity in the aliphatic region (Wei et al., 2005). Aromaticity is the ratio of aromatic compounds to the sum of aromatic and aliphatic compounds. Aromaticity of a

mudrock or isolated kerogen sample can vary from zero to one. It increases as the relative amount of aromatic compounds increases. Figure 10 shows the solid-state ^{13}C NMR spectroscope employed in this research.

Figure 10: Solid-state ^{13}C NMR spectroscope of the NMR Facility at Texas A&M University.

2.5 Electrical Resistivity

To quantify the electrical resistivity of non-heated and heat-treated mudrock and isolated kerogen samples, a high resistance electrometer is used. Figure 11 shows the high resistance electrometer employed in this research, which is capable of measuring a voltage up to 200 V with an input impedance exceeding 200 TΩ. The electrometer applies a preset potential difference to a compacted mudrock or isolated kerogen disk and then measures the resulting current. It applies the alternate polarity technique with 50 volts and 10 seconds for measurement time. Next, Ohm's law is used to calculate the resistance of the

disk. Lastly, I use the dimensions (i.e., thickness and cross-sectional area) of the disk to obtain its resistivity. All resistivity values are measured at room temperature (76 ± 2°F).

Figure 11: High resistance electrometer of W. D. Von Gonten Laboratories.

2.6 Kerogen Density

I measure the density of each isolated kerogen sample with a gas pycnometer. Gas pycnometry is a reliable technology for measuring the density of porous solids. Figure 12 shows the gas pycnometer employed in this research. Figure 13 illustrates the workflow designed in this thesis for assessing kerogen density. The step-by-step gas displacement technique applied by the gas pycnometer includes (a) sealing a sample inside a 10 cm^2 chamber, (b) flowing helium gas into the chamber to fill all accessible voids, (c) allowing the chamber to reach equilibrium, (d) flowing the helium gas from the first chamber into a second chamber, and (e) allowing the second chamber to reach equilibrium. Pressure inside both chambers are monitored at all times by the pycnometer. Each chamber reaches

equilibrium when the change in pressure is less than 0.0050 psig/minute. The outcome of the gas displacement technique is the volume of the sample, which is derived from Boyle's law. Boyle's law enables the calculation of the volume occupied by the helium gas inside the first chamber and thus, the volume of the sample. The gas pycnometer uses the inputted mass and measured volume of the sample to obtain the density of the sample.

The measured density values of the isolated kerogen samples do not represent the true density of kerogen because the products of the isolation procedure contain small amounts of iron disulfide solids. It is necessary to correct the density measurements for the impact of pyrite. To correct the density measurements, I first quantify the weight concentrations of iron (Fe) and sulfur (S) in each isolated kerogen sample with XRF analysis. I then calculate the weight concentration of FeS_2 in each sample. Next, I assume that the density of the FeS_2 solids can range from 4.88 to 5.02 g/cm^3. This assumption allows for the calculation of the volumetric concentration of pyrite in the sample. The estimated volumetric concentration of pyrite enables correcting the density measurements for the impact of pyrite to estimate the true density of kerogen embedded in each organic-rich mudrock formation.

Figure 12: Gas pycnometer of W. D. Von Gonten Laboratories.

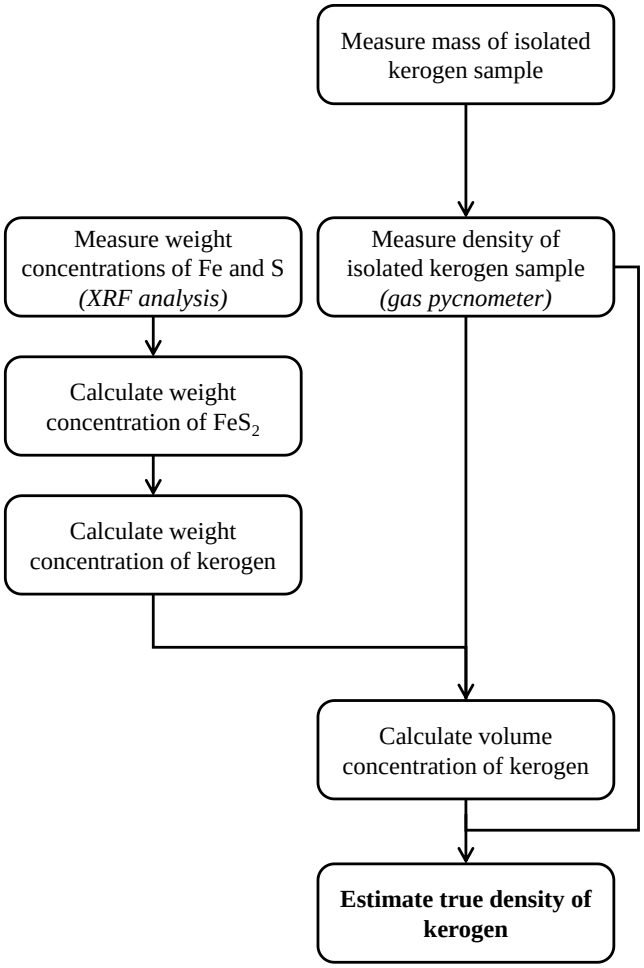

Figure 13: The designed workflow to estimate true density of kerogen.

3. RESULTS[*]

This section presents the results on the effects of thermal maturity on aromaticity, electrical resistivity, and density of kerogen in organic-rich mudrock samples obtained from four formations (i.e., Formation A, B, C, and D). These results include solid-state ^{13}C NMR spectra of powdered mudrock and isolated kerogen samples, electrical resistivity measurements on molded mudrock and isolated kerogen samples, and true density of kerogen embedded in the organic-rich mudrock samples. All mudrock samples are core samples with the exception of those from Formation A, which are outcrop samples.

3.1 Quantifying Thermal Maturity of Mudrock and Isolated Kerogen

To characterize organic matter in mudrock and isolated kerogen samples, geochemical properties acquired from Rock-Eval pyrolysis are used. Specifically, the geochemical parameter HI, which represents hydrogen richness, is used to quantify the thermal maturity of the mudrock and isolated kerogen samples.

3.1.1 Naturally Matured Mudrock and Isolated Kerogen Samples

Table 1 shows the original HI of organic-rich mudrocks obtained from all four formations as well as kerogen isolated from such formations. In the case of the isolated

[*] Part of the data reported in this section is reprinted from An Experimental Approach to Quantify the Impact of Kerogen Maturity on its Chemical Aromaticity and Electrical Conductivity, presented at the SPWLA 57th Annual Logging Symposium, Reykjavik, Iceland, 25-29 June by Yang, A., and Heidari, Z. Copyright 2016 Anqi Yang and Zoya Heidari. Also, part of the data reported in this section is reprinted from Experimental Quantification of the Impact of Thermal Maturity on Kerogen Density, presented at the SPWLA 57th Annual Logging Symposium, Reykjavik, Iceland, 25-29 June by Yang, A., and Heidari, Z. Copyright 2016 Anqi Yang and Zoya Heidari.

kerogen samples, it is evident that kerogen embedded in the four formations vary significantly in thermal maturation levels.

The difference between the mudrock and isolated kerogen samples is potentially due to the mineral matrix effect. The mineral matrix effect can influence HI values acquired from Rock-Eval pyrolysis in rock samples (Katz, 1983). Thus, demineralizing treatments (e.g., HCl and HF acid treatments) are necessary to ensure reliable quantifications of kerogen thermal maturity. In this thesis, I use HI values of isolated kerogen samples as measures of kerogen thermal maturity. It is expected that HI decreases as kerogen thermal maturity increases through natural and synthetic maturation processes.

Table 1: HI (mg hydrocarbon/g organic carbon) of mudrock and isolated kerogen samples from four organic-rich mudrock formations, A, B, C, and D.

Formation	HI of Isolated Kerogen Samples	HI of Mudrock Samples
A	36	16-17
B	41-53	18
C	416-435	347-355
D	596-609	621-625

3.1.2 Synthetically Matured Mudrock and Isolated Kerogen Samples

To evaluate the effects of the synthetic maturation process, I synthetically mature both mudrock and isolated kerogen samples from Formation A to select heat treatment temperatures (i.e., 150°C, 300°C, 425°C, 500°C, and 650°C). Figure 14 shows HI of non-heated and heat-treated mudrock and isolated kerogen samples from Formation A. In both mudrock and isolated kerogen samples, the results indicate that HI decreases as heat treatment temperature increases. This decreasing trend confirms that kerogen thermal

maturity is synthetically increasing with increasing heat treatment temperatures in heat-treated mudrock and isolated kerogen samples. Additionally, this trend demonstrates that HI can be counted as a dependable parameter to quantify thermal maturity of kerogen. In Figure 14, I also observe that the HI measurements in the mudrock samples are lower than those of the isolated kerogen samples. This observation can be due to the mineral matrix effect.

Figure 15 shows HI (mg hydrocarbon/g organic carbon) of isolated kerogen samples from Formation A as a function of OI (mg carbon dioxide/g organic carbon). It is evident that as heat treatment temperature increases, HI and OI decrease in the isolated kerogen samples. First, oxygen depletion occurs in the isolated kerogen samples through synthetic maturation. Next, hydrogen depletion occurs. These trends are in agreement with the evolution path of kerogen embedded in organic-rich mudrocks through natural maturation (Tissot and Welte, 1984).

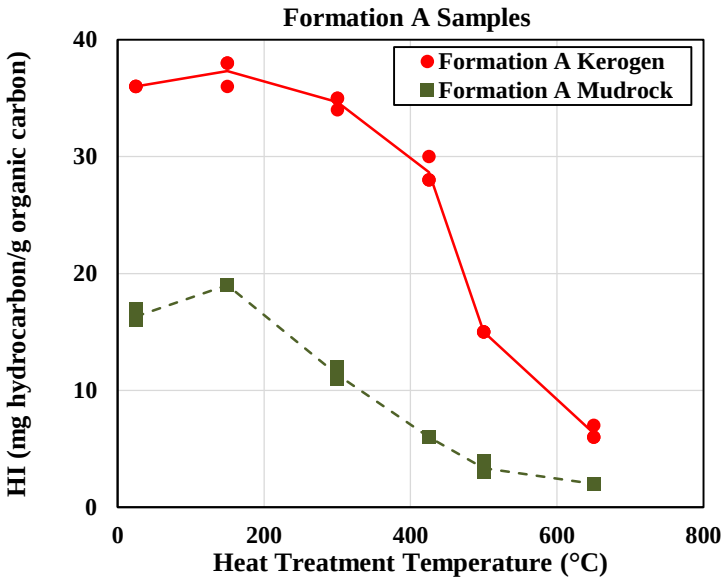

Figure 14: Formation A: HI of mudrock and isolated kerogen samples measured at different heat treatment temperatures.

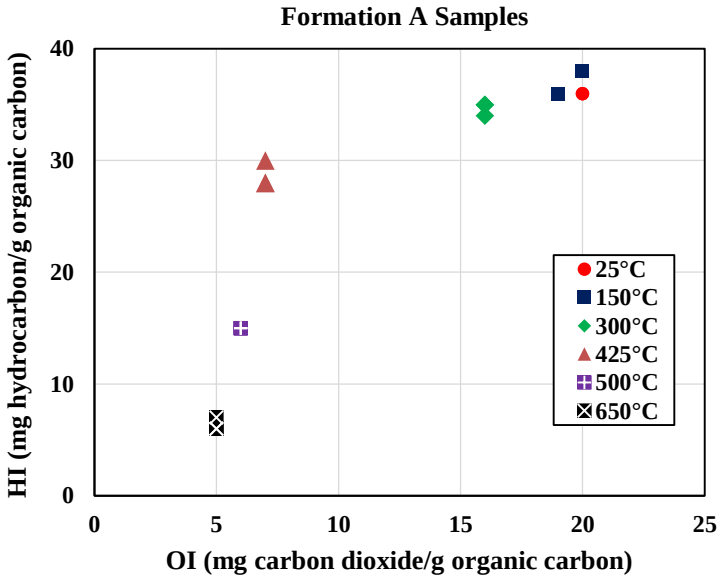

Figure 15: Formation A: HI of isolated kerogen samples as a function of OI.

3.2 Impact of Thermal Maturity on Aromaticity in Mudrock and Isolated Kerogen

To evaluate the effects of thermal maturity on aromaticity, I assess the aromaticity of non-heated and heat-treated mudrock and isolated kerogen samples using solid-state ^{13}C NMR spectroscopy. In each solid-state ^{13}C NMR spectrum, the chemical shifts in parts per million (ppm) of the measured signals identify the compound types (e.g., aromatic and aliphatic compounds). Area under each peak correlates to the relative amount of the identified compound. Relative amounts of aromatic and aliphatic compounds are used to quantify the aromaticity (i.e., f_a) of the analyzed sample.

3.2.1 Naturally Matured Isolated Kerogen Samples

Figure 16 shows the solid-state ^{13}C NMR spectrum of a non-heated kerogen sample from Formation A. HI of this sample is 36 mg hydrocarbon/g organic carbon. Signals in this solid-state ^{13}C NMR spectrum indicate the presence of both aromatic and aliphatic compounds. The high intensity signal at 123.0 ppm indicates the presence of aromatic compounds. The low intensity signal at 20.0 ppm indicates the presence of aliphatic compounds. The relative amount of aromatic compounds is significantly larger than that of aliphatic compounds. The aromaticity of this non-heated kerogen sample is 0.95.

Figure 17 shows the solid-state ^{13}C NMR spectrum of a non-heated kerogen sample from Formation B. HI of this sample is 41 to 53 mg hydrocarbon/g organic carbon. Signals in this solid-state ^{13}C NMR spectrum indicate the presence of both aromatic and aliphatic compounds. The high intensity signal at 127.7 ppm indicates the presence of aromatic compounds. The signals on either side are spinning sidebands. The low intensity

signal at 21.6 ppm indicates the presence of aliphatic compounds. The relative amount of aromatic compounds is significantly larger than that of aliphatic compounds. The aromaticity of this non-heated kerogen sample is 0.92.

Figure 18 shows the solid-state ^{13}C NMR spectrum of a non-heated kerogen sample from Formation C. HI of this sample is 416 to 435 mg hydrocarbon/g organic carbon. Signals in this solid-state ^{13}C NMR spectrum indicate the presence of both aromatic and aliphatic compounds. The signal at 124.0 ppm indicates the presence of aromatic compounds. The signal at 27.0 ppm indicates the presence of aliphatic compounds. The aromaticity of this non-heated kerogen sample is 0.67.

Figure 19 shows the solid-state ^{13}C NMR spectrum of a non-heated kerogen sample from Formation D. HI of this sample is 596 to 609 mg hydrocarbon/g organic carbon. Signals in this solid-state ^{13}C NMR spectrum indicate the presence of both aromatic and aliphatic compounds. The low intensity signals at 135.0 and 119.3 ppm indicate the presence of aromatic compounds. The high intensity signal at 27.5 ppm indicates the presence of aliphatic compounds. The relative amount of aromatic compounds is smaller than that of aliphatic compounds. The aromaticity of this non-heated kerogen sample is 0.40.

Figure 20 shows aromaticity of kerogen isolated from naturally matured organic-rich mudrocks with different origins as a function of HI. The results indicate that in the case of naturally matured kerogen samples, as HI decreases, aromaticity increases. Aromaticity increases from 0.40 to 0.95 as HI decreases from 603 to 36 mg hydrocarbon/g organic carbon. The least thermally matured kerogen is isolated from Formation D and its

aromaticity is 0.40. The most thermally matured kerogen is isolated from Formation A and its aromaticity is 0.95.

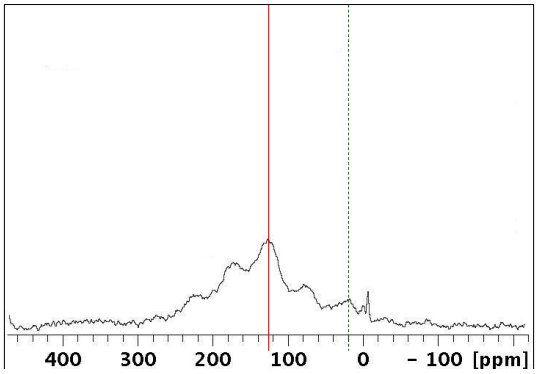

Figure 16: Formation A: solid-state ^{13}C NMR spectrum of a non-heated kerogen sample.

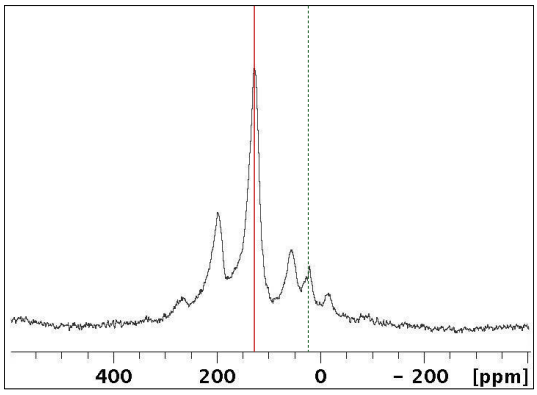

Figure 17: Formation B: solid-state ^{13}C NMR spectrum of a non-heated kerogen sample.

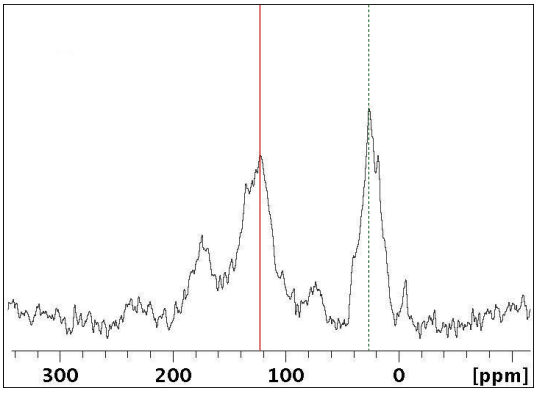

Figure 18: Formation C: solid-state ^{13}C NMR spectrum of a non-heated kerogen sample.

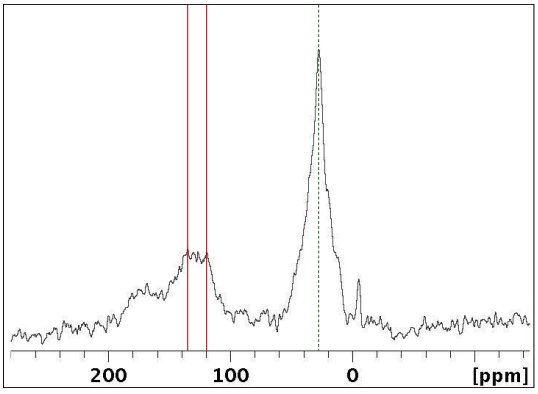

Figure 19: Formation D: solid-state ^{13}C NMR spectrum of a non-heated kerogen sample.

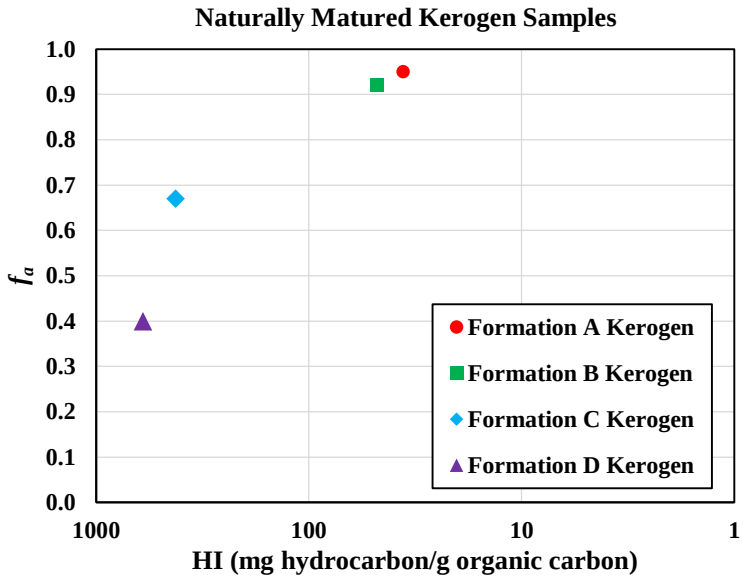

Figure 20: Aromaticity of non-heated kerogen samples from four formations.

3.2.2 Synthetically Matured Isolated Kerogen Samples

Figure 21 shows the solid-state ^{13}C NMR spectrum of a heat-treated kerogen sample from Formation A. HI of this sample is 27 to 32 mg hydrocarbon/g organic carbon. The high intensity signal at 139.0 ppm indicates the presence of aromatic compounds. The aromaticity of this heat-treated kerogen sample is 1.

Figure 22 shows the solid-state ^{13}C NMR spectrum of a heat-treated kerogen sample from Formation B. HI of this sample is 3 mg hydrocarbon/g organic carbon. The high intensity signal at 142.0 ppm indicates the presence of aromatic compounds. The aromaticity of this heat-treated kerogen sample is 1.

Figure 23 shows the solid-state ^{13}C NMR spectrum of a heat-treated kerogen sample from Formation C. HI of this sample is 32 to 45 mg hydrocarbon/g organic carbon. The high intensity signal at 127.0 ppm indicates the presence of aromatic compounds. The

low intensity signals at 48.0 and 22.0 ppm indicate the presence of aliphatic compounds. The relative amount of aromatic compounds is significantly larger than that of aliphatic compounds. The aromaticity of this heat-treated kerogen sample is 0.94.

Figure 24 shows the solid-state ^{13}C NMR spectrum of a heat-treated kerogen sample from Formation D. HI of this sample is 2 mg hydrocarbon/g organic carbon. The high intensity signal at 150.0 ppm indicates the presence of aromatic compounds. The low intensity signals at 39.8 and 30.3 ppm indicate the presence of aliphatic compounds. The relative amount of aromatic compounds is significantly larger than that of aliphatic compounds. The aromaticity of this heat-treated kerogen sample is 0.98.

Figure 25 shows aromaticity of non-heated and heat-treated kerogen samples isolated from organic-rich mudrocks with different origins as a function of HI. Data points representing heat-treated kerogen samples are outlined in black. The results suggest that HI and aromaticity of the isolated kerogen samples decreases and increases, respectively, through synthetic maturation.

In cases of kerogen isolated from organic-rich mudrocks, results from solid-state ^{13}C NMR spectroscopy indicate that the aromaticity of kerogen increases with heat treatments. Through thermal maturation, the increase in kerogen aromaticity is due to two reasons, (a) detachment of alkyl carbons which generates hydrocarbons and (b) aromatization reactions which increase the aromatic cluster size of kerogen (Patience et al., 1992). The latter phenomenon occurs during petroleum generation (Patience et al., 1992) and can continue to occur after aromaticity reaches unity. Aromatization reactions

can increase aromatic cluster size and aromaticity in kerogen by forming new aromatic rings and joining existing and newly formed aromatic carbons with bridgehead carbons.

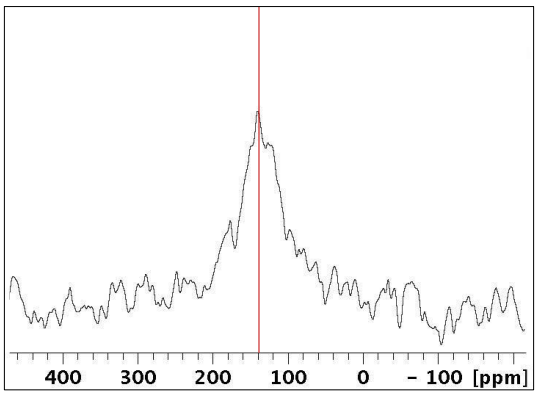

Figure 21: Formation A: solid-state ^{13}C NMR spectrum of a heat-treated kerogen sample.

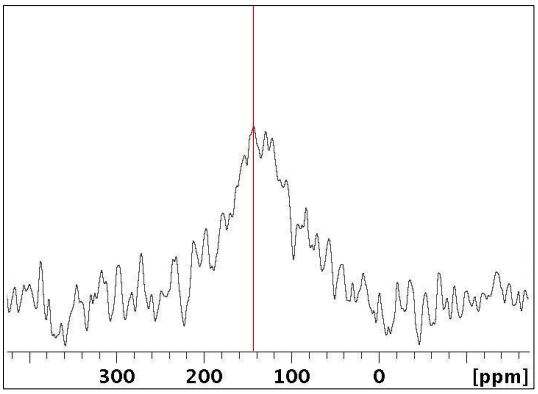

Figure 22: Formation B: solid-state ^{13}C NMR spectrum of a heat-treated kerogen sample.

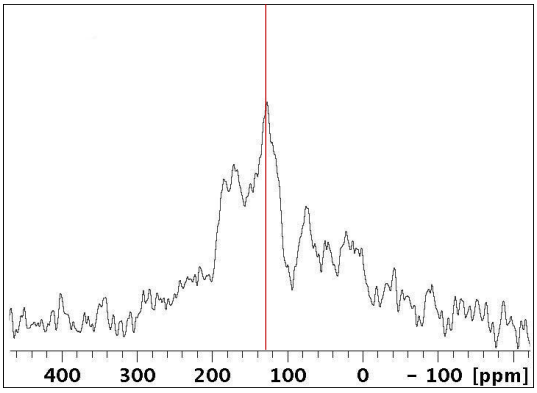

Figure 23: Formation C: solid-state ^{13}C NMR spectrum of a heat-treated kerogen sample.

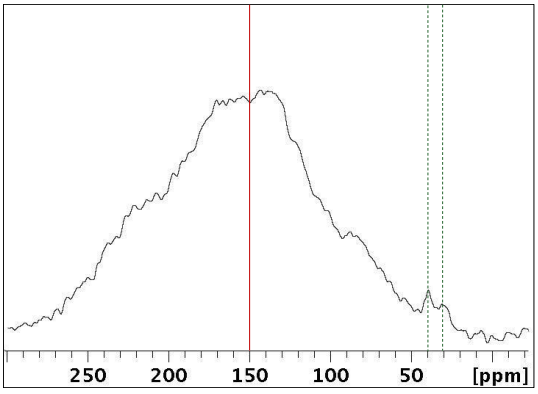

Figure 24: Formation D: solid-state ^{13}C NMR spectrum of a heat-treated kerogen sample.

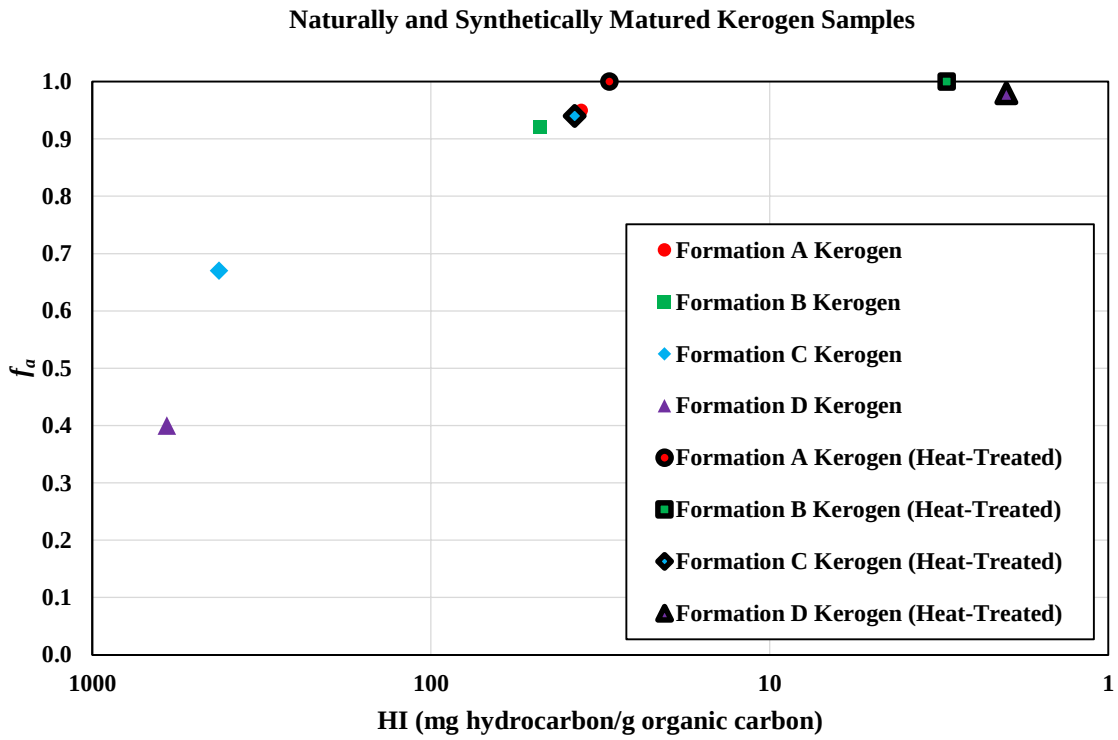

Figure 25: Aromaticity of non-heated and heat-treated kerogen samples from four formations.

3.2.3 Naturally Matured Mudrock Samples

Figure 26 shows the solid-state ^{13}C NMR spectrum of a non-heated mudrock sample from Formation A. HI of this sample is 16 to 17 mg hydrocarbon/g organic carbon. Signals in this solid-state ^{13}C NMR spectrum indicate the presence of both aromatic and aliphatic compounds. The high intensity signal at 126.3 ppm indicates the presence of aromatic compounds. The low intensity signals at 49.5, 30.4, and 17.7 ppm indicate the presence of aliphatic compounds. The relative amount of aromatic compounds is

significantly larger than that of aliphatic compounds. The aromaticity of this non-heated mudrock sample is 0.95.

Figure 27 shows the solid-state ^{13}C NMR spectrum of a non-heated mudrock sample from Formation B. HI of this sample is 18 mg hydrocarbon/g organic carbon. Signals in this solid-state ^{13}C NMR spectrum indicate the presence of aromatic compounds, at 169.1 and 127.1 ppm. The aromaticity of this non-heated mudrock sample is 1.

Figure 28 shows the solid-state ^{13}C NMR spectrum of a non-heated mudrock sample from Formation C. HI of this sample is 347 to 355 mg hydrocarbon/g organic carbon. A signal at 159.0 ppm indicates the presence of aromatic compounds. The aromaticity of this non-heated mudrock sample is 1.

Figure 29 shows the solid-state ^{13}C NMR spectrum of a non-heated mudrock sample from Formation D. HI of this sample is 621 to 625 mg hydrocarbon/g organic carbon. Signals in this solid-state ^{13}C NMR spectrum indicate the presence of both aromatic and aliphatic compounds. The low intensity signal at 128.0 ppm indicates the presence of aromatic compounds. The high intensity signal at 26.0 ppm indicates the presence of aliphatic compounds. The relative amount of aromatic compounds is significantly smaller than that of aliphatic compounds. The aromaticity of this non-heated mudrock sample is 0.44.

Figure 30 shows aromaticity of naturally matured organic-rich mudrock samples with different origins as a function of HI. There are no observable trends.

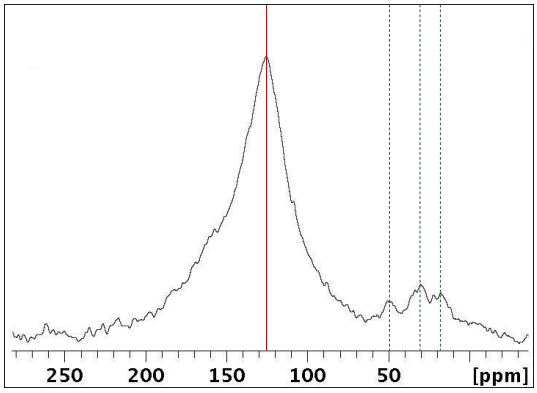

Figure 26: Formation A: solid-state ^{13}C NMR spectrum of a non-heated mudrock sample.

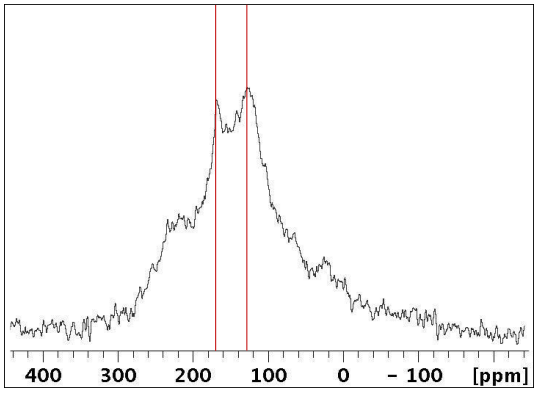

Figure 27: Formation B: solid-state ^{13}C NMR spectrum of a non-heated mudrock sample.

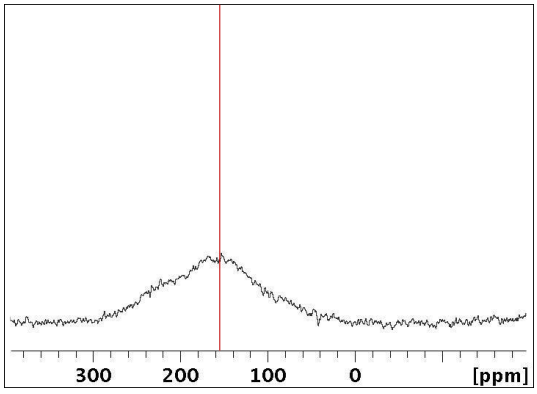

Figure 28: Formation C: solid-state ^{13}C NMR spectrum of a non-heated mudrock sample.

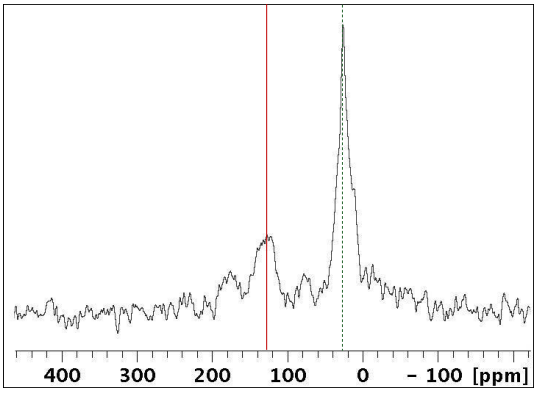

Figure 29: Formation D: solid-state ^{13}C NMR spectrum of a non-heated mudrock sample.

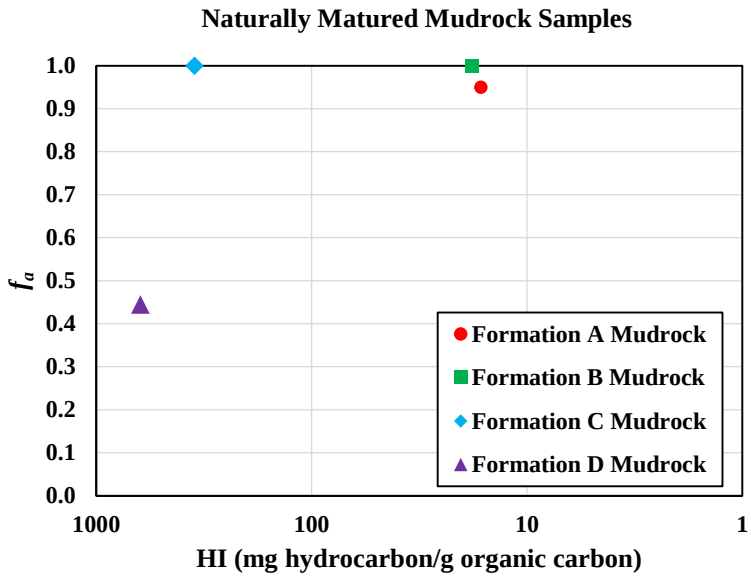

Figure 30: Aromaticity of non-heated mudrock samples from four formations.

3.2.4 Synthetically Matured Mudrock Samples

Figure 31 shows the solid-state ^{13}C NMR spectrum of a heat-treated mudrock sample from Formation A. HI of this sample is 6 mg hydrocarbon/g organic carbon. A

high intensity signal at 148.0 ppm indicates the presence of aromatic compounds. The aromaticity of this heat-treated mudrock sample is 1.

Figure 32 shows the solid-state ^{13}C NMR spectrum of a heat-treated mudrock sample from Formation D. HI of this sample is 95 mg hydrocarbon/g organic carbon. A high intensity signal at 147.0 ppm indicates the presence of aromatic compounds. The aromaticity of this heat-treated mudrock sample is 1.

Figure 33 shows aromaticity of synthetically and naturally matured organic-rich mudrock samples as a function of HI. The aromaticity of all mudrock samples are high with the exception of the non-heated sample from Formation D.

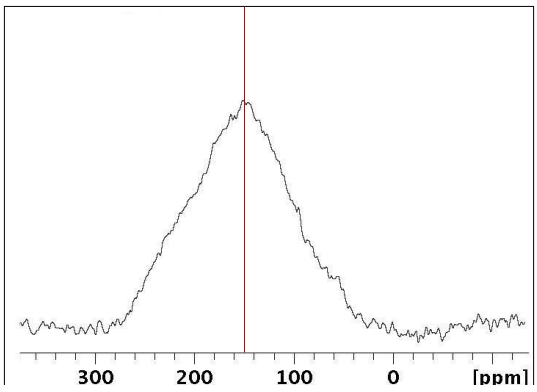

Figure 31: Formation A: solid-state ^{13}C NMR spectrum of a heat-treated mudrock sample.

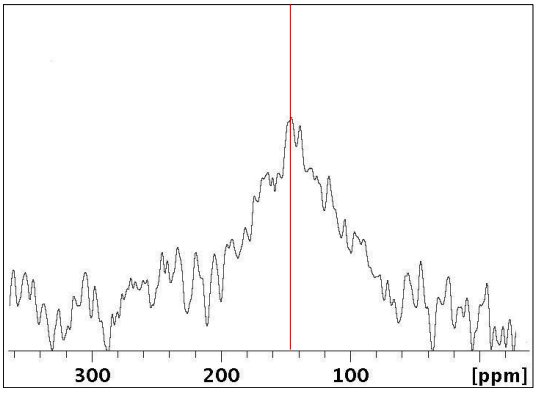

Figure 32: Formation D: solid-state ^{13}C NMR spectrum of a heat-treated mudrock sample.

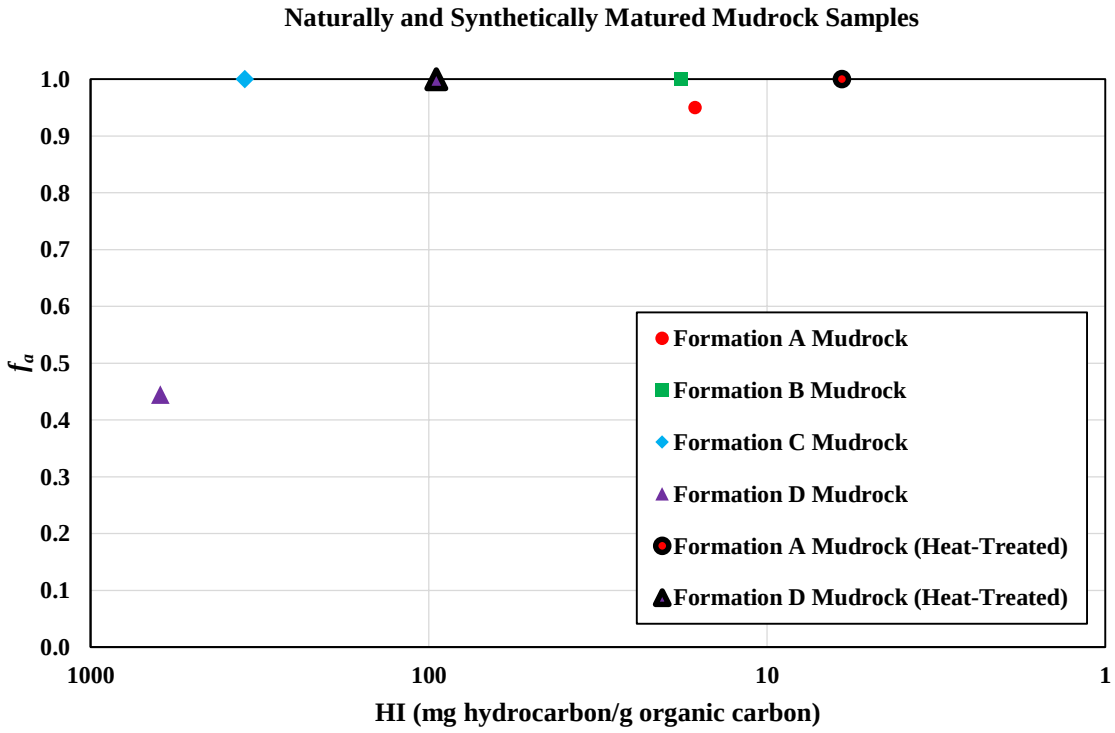

Figure 33: Aromaticity of non-heated and heat-treated mudrock samples from four formations.

3.3 Impact of Thermal Maturity on Electrical Resistivity in Mudrock and Isolated Kerogen

To quantify the impact of thermal maturity on electrical resistivity, I synthetically mature mudrock and isolated kerogen samples from Formation A to select heat treatment temperatures (i.e., 150°C, 300°C, 425°C, 500°C, and 650°C). I then measure electrical resistivity of all samples with a high resistance electrometer.

Figure 34 shows electrical resistivity of non-heated and heat-treated mudrock and isolated kerogen samples from Formation A. In mudrock samples, electrical resistivity increases from 2.32E+7 to 1.07E+8 Ω·m as heat treatment temperature increases from room temperature to 150°C. Resistivity then remains relatively constant (i.e., 1.07E+8 to 1.11E+8 Ω·m) as heat treatment temperature increases to 300°C. As I synthetically mature mudrock samples from 300°C to 650°C, their resistivity values decrease significantly, four orders of magnitude, from 1.11E+8 to 2.09E+4 Ω·m. In isolated kerogen samples, resistivity increases from 2.58E+6 to 1.32E+7 Ω·m as heat treatment temperature increases from room temperature to 150°C. Resistivity then decreases four orders of magnitude from 1.32E+7 to 1.18E+3 Ω·m during synthetic maturation of isolated kerogen samples from 150°C to 650°C. The initial increase in electrical resistivity observed in both mudrock and isolated kerogen samples can be due to the reduction of conductive pathways (e.g., saline water). The significant decrease in resistivity can be due to kerogen aromatization.

In isolated kerogen samples, the decrease in electrical resistivity through synthetic maturation in the range of 150°C to 450°C can be due to increase in the aromaticity of kerogen. Based on results from solid-state ^{13}C NMR spectroscopy (Figure 21) in the heat-treated kerogen sample from Formation A, the aromaticity of kerogen reaches one at 450°C when all aliphatic compounds have converted into aromatic compounds. The decrease in resistivity through synthetic maturation to 650°C can be due to increase in the aromatic cluster size of kerogen. Above 450°C, preexisting and converted aromatic compounds can fuse together to form larger aromatic hydrocarbon molecules, which exhibit a higher tendency towards electron mobility as compared to smaller aromatic hydrocarbon molecules (Northrop and Simpson, 1956). Thus, electrical conductivity in kerogen increases as aromaticity and aromatic cluster size increase in kerogen through synthetic thermal maturation.

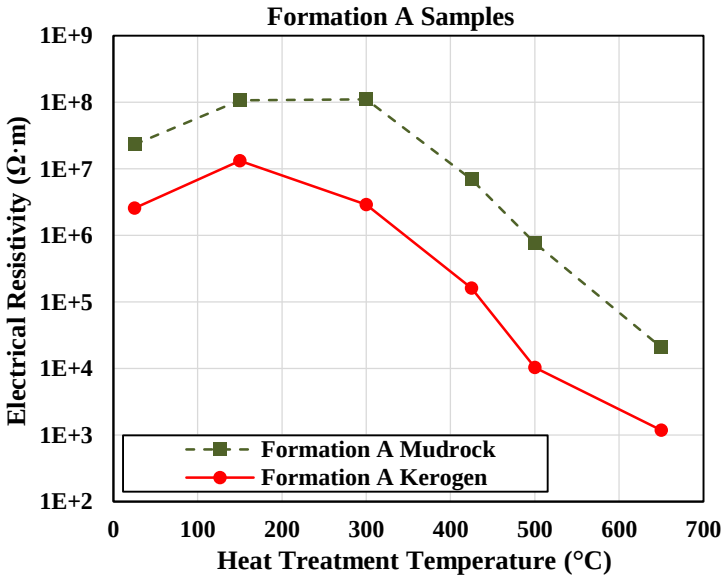

Figure 34: Formation A: Electrical resistivity of mudrock and kerogen samples as a function of heat treatment temperature.

3.4 Impact of Thermal Maturity on Kerogen Density

To investigate the impact of thermal maturity on kerogen density, kerogen samples are isolated from a variety of organic-rich mudrocks. Geochemical properties (e.g., HI and T_{max}) of the isolated kerogen samples are acquired from Rock-Eval pyrolysis. Data collected from XRF analysis and gas pycnometry are used to estimate the true density of each kerogen.

3.4.1 Naturally Matured Isolated Kerogen Samples

Figure 35 shows estimates of the true density of naturally matured kerogen as a function of HI (mg hydrocarbon/g organic carbon) in the four formations, A, B, C, and D. The results demonstrate that kerogen density increases as HI decreases. I also observe a significant variation in kerogen density among organic-rich mudrocks with different origins. The density of kerogen varies from 1.20 to 1.78 g/cm^3 with a variation of 603 to 48 mg hydrocarbon/g organic carbon in HI. Kerogen from Formation A is the least mature and its density is 1.20 g/cm^3. Kerogen from Formation C is the second most mature and its density is 1.78 g/cm^3.

Figure 36 shows the corrected density values of naturally matured kerogen as a function of T_{max} (°C). I do not observe any correlations between T_{max} and the estimated density values. According to Okiongbo et al. (2005), the density of kerogen increases as its T_{max} increases. However, this trend applies only to isolated kerogen samples with T_{max} values higher than 440°C (Okiongbo et al., 2005). T_{max} in three of the samples is less than 440°C and is 441°C in the fourth sample.

Figure 37 shows the true density of kerogen embedded in the four organic-rich mudrock formations as a function of S1 (mg hydrocarbon/g rock). The results indicate that kerogen density increases as S1 decreases. Thus, kerogen density increases as the amount of extractable hydrocarbons in the isolated kerogen samples decrease through natural thermal maturation. It is important to note that multiple chloroform treatments are a part of the kerogen isolation procedure in order to remove free hydrocarbons and bitumen. Thus, S1 detected in the isolated kerogen samples must represent trapped, thermally extractable hydrocarbons. As the amount of these hydrocarbons decreases, kerogen density increases.

Figure 38 shows the true density of kerogen embedded in the four organic-rich mudrock formations as a function of S2 (mg hydrocarbon/g rock). These results demonstrate that the density of kerogen increases as its S2 value decreases. S2 represents the potential of kerogen to generate hydrocarbons (Espitalié et al., 1977). Thus, as the kerogen potential for hydrocarbon generation decreases, its density increases.

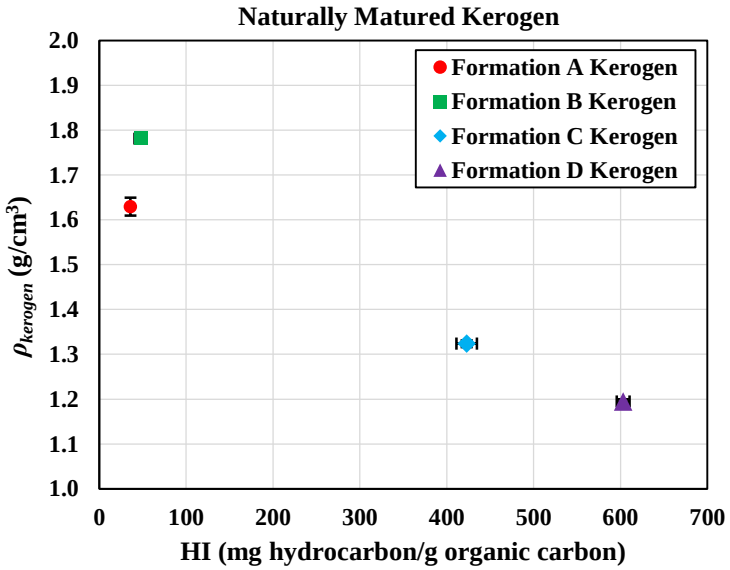

Figure 35: Impact of HI on kerogen density.

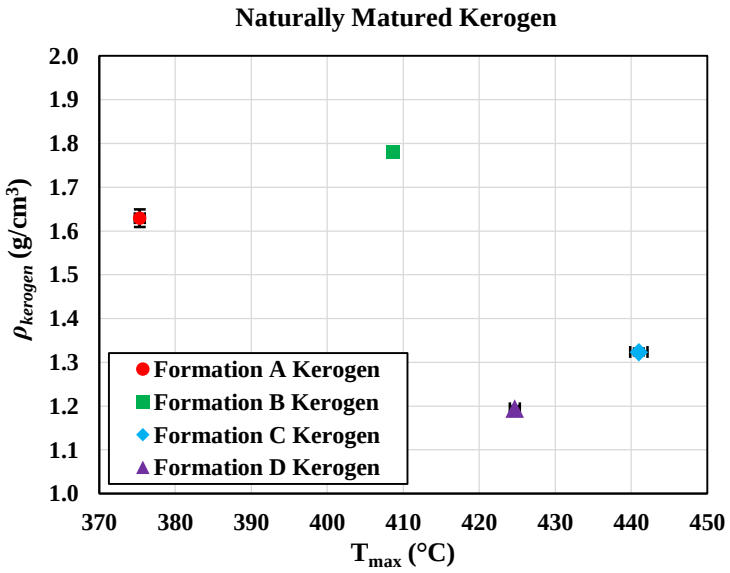

Figure 36: Impact of T_{max} on kerogen density.

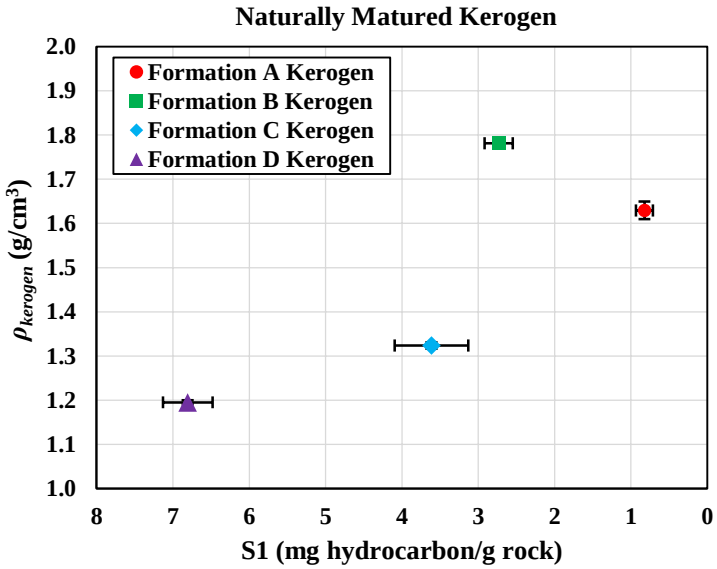

Figure 37: Impact of S1 on kerogen density.

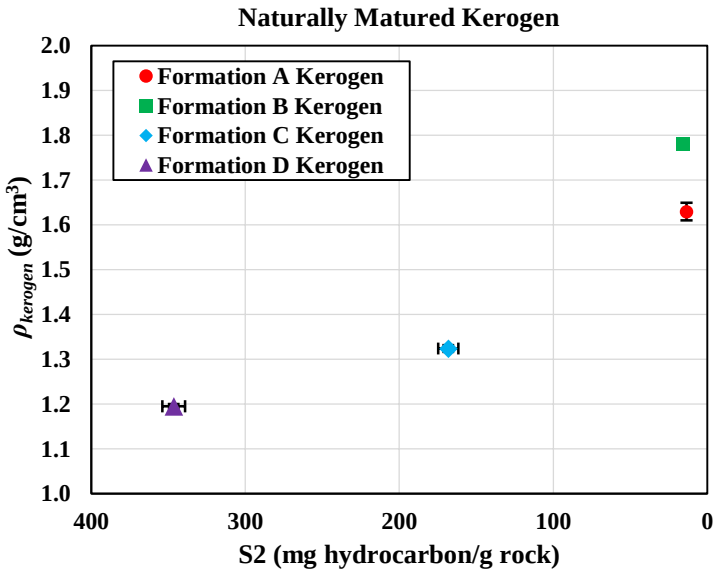

Figure 38: Impact of S2 on kerogen density.

3.4.2 Synthetically Matured Isolated Kerogen Samples

In this subsection, I show estimates of the true density of synthetically matured kerogen from Formation A. Kerogen from Formation A is the least mature one among all isolated kerogen samples. Thus, isolated kerogen samples from Formation A are heat-treated to 300°C, 425°C, 500°C, and 650°C to evaluate the effects of synthetic maturation on kerogen density.

Figure 39 demonstrates the corrected density of non-heated and heat-treated kerogen from Formation A. I plot the density of the non-heated kerogen at 25°C. These results suggest that kerogen density decreases initially and then increases as a function of heat treatment temperature. However, the difference between the highest and the lowest density values is only 0.14 g/cm^3.

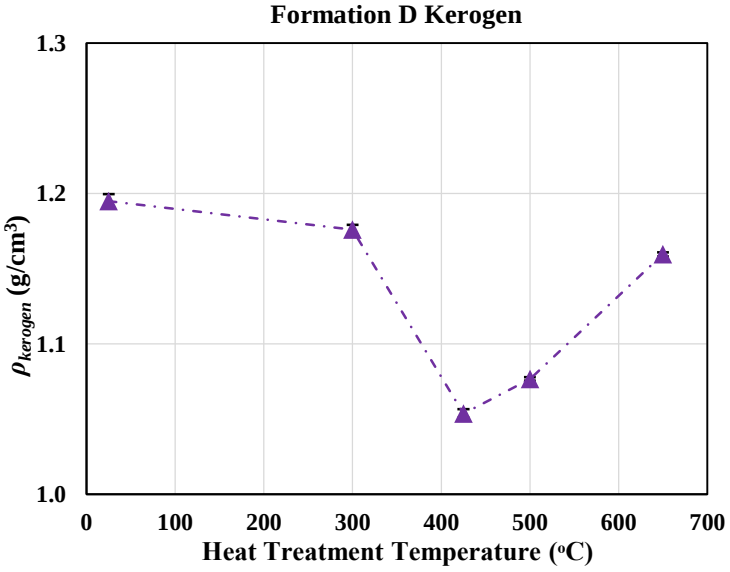

Figure 39: Formation D: Impact of heat treatment temperature on estimated density values of synthetically matured kerogen.

Figure 40 shows HI and T_{max} of non-heated and heat-treated isolated kerogen samples from Formation A as a function of heat treatment temperature (°C). These results show that HI and T_{max} do not vary significantly between the non-heated and heat-treated isolated kerogen samples. The results also suggest that synthetic maturation might not be a reliable representation of natural maturation. Thus, the density values estimated for samples synthetically matured in the laboratory might not be reliable representatives for those samples undergone natural maturation.

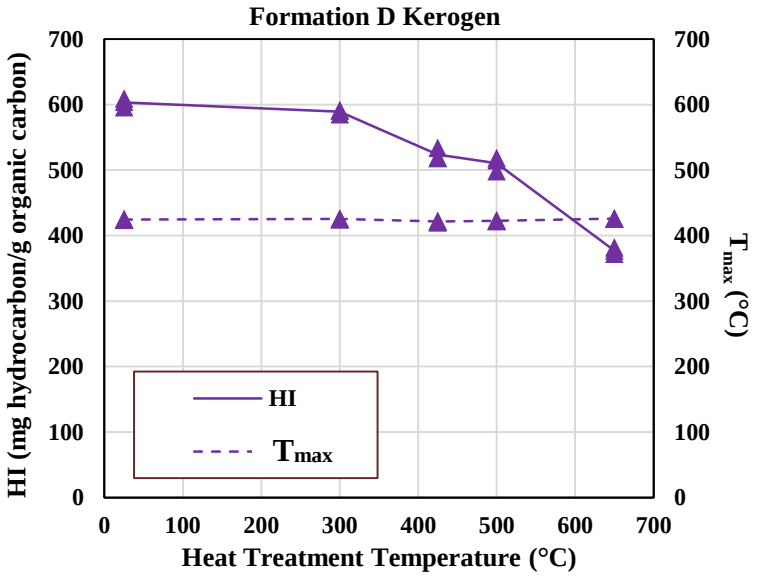

Figure 40: Formation D: Impact of heat treatment temperature on HI and T_{max} of synthetically matured kerogen samples.

3.4.3 Sensitivity Analysis: Effects of Kerogen Density on Porosity and Water Saturation in Organic-Rich Mudrocks

Based on the experimental results, kerogen density varies significantly as a function of thermal maturity (i.e., variation of 36 to 603 mg hydrocarbon/g organic carbon

in HI). I perform a sensitivity analysis to evaluate the effects of a significant variation in the density of kerogen on the estimates of porosity and water saturation in organic-rich mudrocks. I construct a synthetic petrophysical/compositional model of an organic-rich mudrock based on real field examples for the purpose of this sensitivity analysis. The model consists of kerogen, clay and non-clay minerals, water, and hydrocarbon. The mineral components assumed in this model include illite, smectite, chlorite, calcite, dolomite, quartz, and pyrite. Table 2 lists the density and volumetric concentration of kerogen and mineral/fluid components assumed in the petrophysical/compositional model.

Results from the sensitivity analysis demonstrate that 0.58 g/cm^3 increase in the density of kerogen (i.e., from 1.20 to 1.78 g/cm^3) leads to relative errors of 48% and 25% in estimates of porosity and water saturation, respectively. Thus, uncertainty in estimates of kerogen density can cause significant errors in estimates of porosity and water saturation in organic-rich mudrocks.

Table 2: Density and concentration of fluids and mineral components assumed in the petrophysical/composition model considered for sensitivity analysis.

Constituent	**Density (g/cm^3)**	**Concentration**
Illite	2.75	30%
Smectite	2.45	13%
Chlorite	2.76	3%
Calcite	2.71	10%
Dolomite	2.87	8%
Quartz	2.65	19%
Pyrite	5.01	5%
Kerogen	1.20 – 1.78	5%
Hydrocarbon	0.80	4%
Saline Water	1.05	3%

4. SUMMARY AND CONCLUSIONS

This section highlights the contributions of this thesis. It is organized into two subsections, summary and conclusions. The summary subsection first reviews the objectives and then summarizes the results of this thesis. The conclusions subsection discusses the significance of this research.

4.1 Summary

The objectives of this thesis consisted of experimentally quantifying

(a) Aromaticity in isolated kerogen samples,

(b) Electrical resistivity in organic-rich mudrock and isolated kerogen samples, and

(c) Density of kerogen embedded in a variety of organic-rich mudrock samples,

as a function of thermal maturity.

In this thesis, the effects of thermal maturity on aromaticity, electrical resistivity, and density of kerogen were quantified in a variety of organic-rich mudrocks with different origins. To enable direct measurements of chemical, electrical, and physical properties of kerogen, I first isolated kerogen from organic-rich mudrock samples obtained from four formations. Next, I synthetically matured both mudrock and isolated kerogen samples to select heat treatment temperatures in order to evaluate the effects of both natural and synthetic maturation. Next, I characterized thermal maturity using the geochemical parameter HI as derived from Rock-Eval pyrolysis. The chemical structures of mudrock and isolated kerogen samples were then quantified with aromaticity assessed

using solid-state ^{13}C NMR spectroscopy. Next, I directly measured the electrical resistivity of both non-heated and heat-treated mudrock and isolated kerogen molds. I then measured the density of each isolated kerogen sample using a gas pycnometer with helium gas as the displacement medium. I estimated the true density of kerogen embedded in each formation by applying corrections for the impact of pyrite using results from XRF analysis. Lastly, I estimate the true density of heat-treated kerogen from the least mature formation in order to evaluate the effects of synthetic maturation on kerogen density.

Results acquired from solid-state ^{13}C NMR spectra of four formations demonstrated that natural and synthetic maturation led to significant increases in kerogen aromaticity. In the case of naturally matured kerogen samples, aromaticity increased from 0.40 to 0.95 due to a decrease in HI from 603 to 36 mg hydrocarbon/g organic carbon. In the case of synthetically matured kerogen samples, HI and aromaticity of kerogen isolated from each organic-rich mudrock decreased and increased, respectively. In kerogen isolated from Formation A, aromaticity increased 5.3% with a decrease of 4 to 9 mg hydrocarbon/g organic carbon in HI. In kerogen isolated from Formation B, aromaticity increased 8.7% with a decrease of 38 to 50 mg hydrocarbon/g organic carbon in HI. In kerogen isolated from Formation C, aromaticity increased 40.3% with a decrease of 371 to 403 mg hydrocarbon/g organic carbon in HI. In kerogen isolated from Formation D, aromaticity increased 145.0% with a decrease of 594 to 607 mg hydrocarbon/g organic carbon in HI.

High resistance measurements of molded mudrock and isolated kerogen samples from Formation A demonstrated resistivity decreases as a function of thermal maturity. In

molded organic-rich mudrock samples from Formation A, electrical resistivity increased from 2.32E+7 to 1.07E+8 Ω·m as heat treatment temperature increased from room temperature to 150°C. Resistivity then remained relatively constant (i.e., 1.07E+8 to 1.11E+8 Ω·m) as heat treatment temperature increased to 300°C. As the mudrock samples were synthetically matured from 300°C to 650°C, their resistivity values decreased significantly, four orders of magnitude, from 1.11E+8 to 2.09E+4 Ω·m, which corresponded to a decrease in HI of 14 to 15 mg hydrocarbon/g organic carbon. In molded kerogen samples from Formation A, resistivity increased from 2.58E+6 to 1.32E+7 Ω·m as heat treatment temperature increased from room temperature to 150°C. Resistivity then decreased four orders of magnitude from 1.32E+7 to 1.18E+3 Ω·m as the molded kerogen samples were synthetically matured from 150°C to 650°C, while HI decreased 29 to 30 mg hydrocarbon/g organic carbon. The initial increase in electrical resistivity observed in both organic-rich mudrock and isolated kerogen samples can be due to the reduction in the amount of conductive pathways (e.g., saline water). The significant decrease in resistivity can be caused by the aromatization of kerogen. It should be noted that all resistivity measurements were performed at room temperature (76 ± 2°F). Thus, electrical properties of kerogen at subsurface temperatures might be different than those measured in the laboratory.

Results acquired from gas pycnometer and XRF analysis on four organic-rich mudrock formations demonstrated that thermal maturity has a significant impact on kerogen density. As kerogen thermally matures, its density increases. I observed a variation in kerogen density from 1.20 to 1.78 g/cm^3 when HI varied in the range of 603

to 48 mg hydrocarbon/g organic carbon. Uncertainty in quantifying kerogen density can influence the accuracy of well-log-based estimates of petrophysical properties (i.e., porosity and water saturation). Furthermore, I observed that density estimations in the synthetically matured samples were not in agreement with the ones in the naturally matured samples. Results obtained from heat-treated isolated kerogen samples suggested that synthetic maturation might not be considered as a reliable substitute for the natural maturation process in the case of density evaluation.

4.2 Conclusions

To potentially improve the dependability of well-log-based petrophysical evaluation of organic-rich mudrocks, it is essential to better understand chemical, electrical, and physical properties of thermally matured kerogen. The documented experimental results in this thesis contribute to this ongoing effort. In this thesis, aromaticity, electrical resistivity, and density of kerogen embedded in a variety of organic-rich mudrock were quantified. The results on resistivity can potentially contribute to the development of models to improve the interpretation of electrical resistivity measurements for reliable assessment of in-situ hydrocarbon saturation. The results on density can potentially improve the interpretation of bulk density measurements for reliable assessments of porosity and water saturation. According to the documented sensitivity analysis, 0.58 g/cm^3 increase in the density of kerogen led to significant relative errors in estimates of porosity (i.e., 48%) and water saturation (i.e., 25%). Thus, reliable estimates

of kerogen density after taking into account its thermal maturity can potentially improve well-log-based evaluation of porosity and water saturation in organic-rich mudrocks.

REFERENCES

Baskin, D.K., 1997, Atomic H/C Ratio of Kerogen as an Estimate of Thermal Maturity and Organic Matter Conversion, *AAPG Bulletin*, **81**(9), 1437-1450.

Clementz, D.M., 1978, Effect of Oil and Bitumen Saturation on Source-Rock Pyrolysis, *AAPG Bulletin*, **63** (12), 2227-2232.

Dellisanti, F., Pini, G.A., and Baudin, F., 2010, Use of T_{max} as a Thermal Maturity Indicator in Orogenic Successions and Comparison with Clay Mineral Evolution, *Clay Minerals*, **45**, 115-130.

Duba, A.G., 1983, Electrical Conductivity of Colorado Oil Shale to 900°C, *Fuel*, **62**, 966-972.

Durand, B., 1980, *Kerogen: Insoluble Organic Matter from Sedimentary Rocks*, Éditions Technip, Paris, 13-34.

Durand, B., and Nicaise, G., 1980, *Kerogen: Insoluble Organic Matter from Sedimentary Rocks*, Éditions Technip, Paris, 35-52.

Ebukanson, E.J., and Kinghorn, R.R.F., 1985, Kerogen Facies in the Major Jurassic Mudrock Formations of Southern England and the Implication on the Depositional Environments of Their Precursors, *Journal of Petroleum Geology*, **8**(4), 435-462.

Espitalié, J., Madec, M., Tissot, B., Mennig, J.J., and Leplat, P., 1977, Source Rock Characterization Method for Petroleum Exploration, Paper OTC-2935, presented at the Offshore Technology Conference, Houston, Texas, USA, 2-5 May.

Espitalié, J., Madec, M., and Tissot, B., 1980, Role of Mineral Matrix in Kerogen Pyrolysis: Influence on Petroleum Generation and Migration, *AAPG Bulletin*, **64** (1), 59-66.

Firdaus, G., and Heidari, Z., 2015, Quantifying Electrical Resistivity of Isolated Kerogen from Organic-Rich Mudrocks Using Laboratory Experiments, Paper SPE-175078, presented at the SPE Annual Technical Conference and Exhibition, Houston, Texas, USA, 28-30 September.

Horsfield, B., and Douglas, A.G., 1980, The Influence of Minerals on the Pyrolysis of Kerogens, *Geochimica et Cosmochimica Acta*, **44**, 1110-1131.

Katz, B.J., 1983, Limitations of 'Rock-Eval' Pyrolysis for Typing Organic Matter, *Organic Geochemistry*, **4**(3), 195-199.

Kinghorn, R.R.F., and Rahman, M., 1980, The Density Separation of Different Maceral Groups of Organic Matter Dispersed in Sedimentary Rocks, *Journal of Petroleum Geology*, **2**(4), 449-454.

Kinghorn, R.R.F., and Rahman, M., 1983, Specific Gravity as a Kerogen Type and Maturation Indicator with Special Reference to Amorphous Kerogens, *Journal of Petroleum Geology*, **6**(2), 79-194.

Klemme, H.D., and Ulmishek, G.F., 1991, Effective Petroleum Source Rocks of the World: Stratigraphic Distribution and Controlling Depositional Factors, *AAPG Bulletin*, **75** (12): 1809-1851.

Jarvie, D.M., 1991, *Source and Migration Processes and Evaluation Techniques*, AAPG Press, Tulsa, 113-118.

Mao, J., Fang, X., Lan, Y., Schimmelmann, A., Mastalerz, M., Xu, L., and Schmidt-Rohr, K., 2010, Chemical and Nanometer-Scale Structure of Kerogen and Its Change during Thermal Maturation Investigated by Advanced Solid-State ^{13}C NMR Spectroscopy, *Geochimica et Cosmochimica Acta*, **74**, 2110-2127.

Meng, D., Ma, T., Geng, C., and Sun, Y., 2012, Test Method and Experimental Research on Resistance of Oil Shale under High Temperature, *Global Geology*, **15**, 245-251.

Nordeng, S.H., 2012, Basic Geochemical Evaluation of Unconventional Resource Plays, *Geo News*, **39**, 14-18.

Northrop, D.C., and Simpson, O., 1956, Electronic Properties of Aromatic Hydrocarbons, *Royal Society Publishing*, **234**(1196), 124-135.

Patience, R.L., Mann, A.L., and Poplett, I.J.F., 1992, Determination of Molecular Structure of Kerogen Using ^{13}C NMR Spectroscopy: III. The Effects of Thermal Maturation on Kerogens from Marine Sediments, *Geochimica et Cosmochimica Acta*, **56**, 2725-2742.

Peters, K.E., 1986, Guidelines for Evaluating Petroleum Source Rock Using Programmed Pyrolysis, *AAPG Bulletin*, **70**, 318-329.

Rajeshwar, K., Das, M., and DuBow, J., 1980, D.C. Electrical Conductivity of Green River Oil Shales, *Nature*, **287**, 131-133.

Tissot, B., Durand, B., Espitalié, J., and Combaz, A., 1974, Influence of Nature and Diagenesis of Organic Matter in Formation of Petroleum, *AAPG Bulletin*, **58**(3), 499-506.

Tissot, B., and Welte, D., 1984, *Petroleum Formation and Occurrence*, Springer-Verlag, Berlin, Heidelberg, New York, Tokyo.

Vandenbroucke, M., 2003, Kerogen: From Types to Models of Chemical Structure, *Oil & Gas Science and Technology*, **58**(2), 243-269.

Vandenbroucke, M., and Largeau, C., 2007, Kerogen Origin, Evolution and Structure, *Organic Geochemistry*, **38**(5), 719-833.

Van Krevelen, D.W., 1961, *Coal*, Elsevier, London.

Walters, C.C., Kliewer, C.E., Awwiller, D.N., Rudnicki, M.D., Passey, Q.R., and Lin, M.W., 2014, Influence of Turbostratic Carbon Nanostructures on Electrical Conductivity in Shales, *International Journal of Coal Geology*, **122**, 105-109.

Wei, Z., Gao, X., Zhang, D., and Da, J., 2005, Assessment of Thermal Evolution of Kerogen Geopolymers with Their Structural Parameters Measured by Solid-State ^{13}C NMR Spectroscopy, *Energy & Fuel*, **19**, 240-250.